Control Design for an Energy-Sharing Module of Next-Generation Thermal Energy System ectogrid™

Lisa Korsell

Tuva Ydén

LUND UNIVERSITY

Department of Automatic Control

MSc Thesis
TFRT-6131
ISSN 0280-5316

Department of Automatic Control
Lund University
Box 118
SE-221 00 LUND
Sweden

Printed in Sweden by Tryckeriet i E-huset
Lund 2021

Abstract

Today, heat and electricity production are two main sources of greenhouse gas emissions. A big share of the overall energy consumption is used to provide buildings with heating and cooling. Smart-energy solutions of heating and cooling could therefore be a more sustainable solution contributing to the green transition of the energy system. ectogrid™ is a new generation of a cooperative heating and cooling network providing buildings with energy in an efficient way. Compared to traditional energy solution such a district heating and heat pump/chillers, ectogrid™ is a smart-energy solution utilizing low-temperature heat which is usually wasted.

Every building connected to ectogrid™ has its own production module equipped with a heat pump or a chiller supplying the building with heating or cooling. To meet the required demand in the buildings and to maintain desired grid temperatures, the flow of water from the grid into each building is controlled using a circulation pump and control valve. The network consists of an interconnection of energy-sharing modules affecting each other, therefore it is of importance that the grid temperature lies within a defined temperature range for the network to work efficiently. Today, flow control into a module is currently done using a manually tuned PI-controllers. The objective of this thesis is to improve flow control into one energy-sharing module and to develop a method to tune the controllers for new buildings.

A simulation model over one energy-sharing module equipped with a heat pump was developed using Matlab Simulink®. The model was used as a pre-study for evaluating control tuning methods. Control performances were evaluated on the controller's ability to reject disturbances affecting outgoing temperature as well as the overall stability. The result from the pre-study was used as support for controller testing in real buildings. This resulted in a generic way to tune new buildings connected to the grid, based on lambda-tuning method. The PI-controller is limited regarding disturbance rejection while maintaining stability. Therefore, the possibility to implement a feedforward was investigated using the simulation model. Since

feedforward showed great potential in reducing the impact of disturbances this was suggested as a future outlook.

Acknowledgements

We wish to thank various people for their contribution to this project. A special thanks to our supervisors Pauline Kergus and Felix Agner at the Automatic Control department. They have been very helpful and encouraging during the project. No matter what, they have always taken their time to discuss thoughts and ideas. We have also very much appreciated the input from Tore Hägglund, we would like to thank him for being supportive and for sharing his knowledge about automatic control and tuning of PI-controllers. Finally, thanks to our examiner Anders Rantzer.

We would also like to thank the people from E.ON ectogrid™, especially our supervisor Daniel Stenberg for the support and help during the project. Also, we are very grateful for all the help and technical guidance from Thomas Ranstorp.

Contents

1. Introduction **9**
- 1.1 General Background on Heating and Cooling Networks 9
- 1.2 Description of ectogrid™ 10
- 1.3 Description of ectocloud™ 13
- 1.4 Objective 13
- 1.5 Outline of Report 14

2. Modelling of an Energy-Sharing Module **15**
- 2.1 Overview of an Energy-Sharing Module 15
- 2.2 Actuator Characteristics and Allocation Strategy 23
- 2.3 Circulation Pump 27
- 2.4 Control Valve 30
- 2.5 Heat Pump 32
- 2.6 Closed-loop 37

3. Flow Control of Energy-Sharing Modules **43**
- 3.1 Control Specifications 43
- 3.2 Performance Evaluation Methods 44
- 3.3 Controller Tuning 46
- 3.4 Pre-study using Simulations 48
- 3.5 Testing Control Performance in Building 303 55
- 3.6 Impact of Control Parameters 59
- 3.7 Improved Tuning Method 60
- 3.8 Simulation of Improved Tuning Method 61
- 3.9 Verification of New Tuning Method in Building 303 65

4. Conclusions and Outlooks **68**
- 4.1 Method for Future Controller Tuning 68
- 4.2 Discussion 69
- 4.3 Outlooks 72
- 4.4 Conclusion 78

Bibliography **79**

A. Matlab Simulink® 82

B. Simulation Model of an Energy-Sharing Module with a Chiller 84

C. Project activities 88

C.1 Workshop 16/3-2021 88

C.2 Testing in Real Buildings 88

1

Introduction

1.1 General Background on Heating and Cooling Networks

Climate change is the biggest threat against our planet's future. Therefore, our generation stands in front of a great challenge, adjusting to a sustainable way of living. To avoid a climate catastrophe, a drastic reduction of greenhouse gas emissions is needed [Team et al., 2014]. According to the IPCC (Intergovernmental Panel on Climate Change), heat production and electricity production is one of the main sources of greenhouse gas emissions. To face this challenge, the energy systems should allow increasing the share of renewable energy sources. Another strategic axis consists in proposing more efficient uses of energy.

In this context, heating and cooling of buildings plays an important role in the energy system. In Sweden half of the use of energy in the building- and service sector is used for heating and cooling [Energimyndigheten, 2020]. Smart energy solutions for waste heating and cooling could therefore play an important role in adjusting to a sustainable and more efficient energy system. Today, most cities in Sweden are provided with heat from district heating networks [Forslund and Forslund, 2016], district heating networks are high-temperature networks (65-115^{o}C) supplying buildings with heat. It is a great way to increase the the use of high temperature waste energy. Outside of cities transmission losses are too large to keep an efficient use of district heating [Buffa et al., 2019]. Thus, heat pumps powered by electricity are commonly used in areas outside district heating networks [Forslund and Forslund, 2016]. Actually, this is the most common heat source in small houses [Energimyndigheten, 2020]. Regarding cooling, buildings are mainly provided with cooling from chillers or free-cooling, where free-cooling is a cooling network using the same principle as district heating. Traditional chillers use electricity but also refrigerants, which are usually environmentally hazardous [Forslund and Forslund, 2016].

To increase the efficiency of energy usage, it would be favourable if the use of low-

temperature waste heat is increased, as a large amount of low-temperature heat is available and wasted [Rezaie and Rosen, 2012]. There are several advantages utilizing a low-temperature energy network compared to traditional district heating and cooling networks. Due to the small temperature difference between the ground and pipes, there is a small loss of thermal energy. With this type of energy network, high flexibility can be achieved. The system can as well be combined and integrated with the high-temperature district heating networks. It also allows recovering different types of excess heat, which is important for increasing efficient use of energy [Buffa et al., 2019].

One solution utilizing a low-temperature network is a smart-energy solution called ectogrid™. ectogrid™ uses already existing technologies, heat pumps, cooling machines and distribution and favourably combines them. This solution contributes to the use of low-temperature excess heating and cooling, which is more efficient by avoiding large energy losses compared to large-scale production. Besides, ectogrid™ introduces an extra dimension of flexibility in the energy system by balancing neighbour thermal energy flows [Ectogrid, 2021]. In this master thesis, the focus will be on the world's first ectogrid™ placed in Medicon Village in Lund. The objective is to improve flow control into a building to maintain desired temperatures on the grid.

1.2 Description of ectogrid™

ectogrid™ is a new generation of cooperative heating and cooling networks. It combines both small-scale production with features of large-scale distribution, such as traditional district heating and cooling networks. Figure 1.1 describes the structure of ectogrid™. The main components are:

- A warm pipe and a cold pipe connecting buildings.
- Energy-sharing modules in every building connected to the grid, either consisting of heat pumps or chillers.
- An active balance unit providing the grid with extra heating and cooling.
- A passive balance unit providing energy balance flexibility between the warm and cold pipes as well as hydraulic balance on the grid.

Energy production is performed with heat pumps and chillers powered by electricity, located in every building connected to the grid. This part is called an energy-

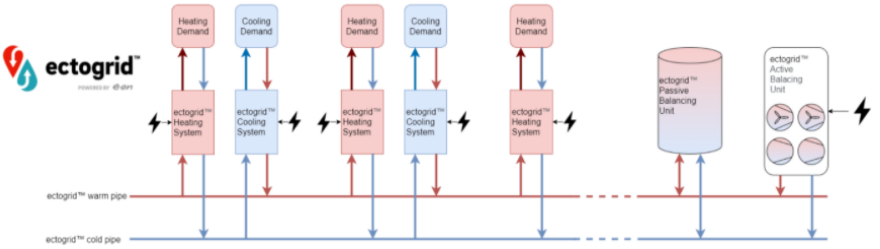

Figure 1.1: General picture over ectogrid™.

sharing module. ectogrid™ uses the excess energy[1] from each energy-sharing module, which is shared on a common grid with one warm and one cold pipe. The warm pipe is fed with excess heat and the cold pipe with excess cooling. The warm and cold pipes are further used to provide all energy-sharing modules with hot or cold water to match their specific demand for heating or cooling. By matching heating and cooling demands, the usage of heat pumps and therefore the subsequent usage of electrical power can be minimized. The temperatures on the grid are balanced by the overall heating and cooling demand. ectogrid™ consists of one passive balancing unit and one active balancing unit which are used to help to balance the heating and cooling demand. The temperature range on the grid is normally 16-40°C for the warm pipe and 6-30°C for the cold pipe.

For ectogrid™ to work efficiently, it is important that the temperatures on the grid lie within a defined range. This is because the heat pumps and chillers require specific inlet temperatures to work efficiently. An example is when inlet temperature lies under the desired inlet temperature of the heat pump. Then the efficiency of the heat pump is reduced. The efficiency is determined by the coefficient of performance (COP) which is defined as the ratio between heat leakage into the system and compressor input [Eastop and McConkey, 1993]. When the inlet temperature is too low, less heat is transferred into the system, which results in lower COP. Therefore, if the heat pump should perform well it is of importance that the inlet temperature is kept at the desired set-point. Otherwise, the performance of heat pumps and chillers is reduced and they might not be able to produce enough heating or cooling for the buildings connected to the grid. If the outlet temperature from one unit fluctuates, this will have a direct impact on the inlet temperature in the next building.

To maintain a specific return temperature to the grid, the inlet flows from ectogrid™

[1] Excess energy: As a result of heating production of an ectogrid™ heating module to meet a specific demand, cooling is also produced as a by-product and vice versa for an ectogrid™ cooling module. This excess energy is shared on the common grid to help fulfill other demands rather than going waste.

into an energy-sharing module is controlled according to the physical relationship between energy transfer, flow, and temperature difference. The general structure of one energy-sharing module is presented in Figure 1.2a and Figure 1.2b. A unit consisting of a heat pump providing the building with heat is denoted VP and a unit consisting of a chiller providing the building with cooling is denoted KP. To meet the required heating or cooling demand in the building, compressors in the heat pump are stepping in and out. This has a severe effect on the outgoing temperatures to the grid. Therefore, this creates a need for flow control into each module. Compared to a traditional district heating and cooling system ectogrid™ utilizes internal circulation pumps. The pumps are located at each energy-sharing module to drive flow on the grid. Therefore, the net flow of each module contributes to the total flow and pressure in the whole system.

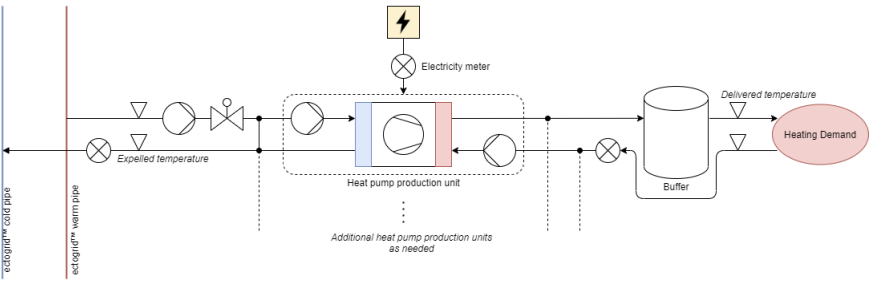

(a) An energy-sharing module providing the building with heat

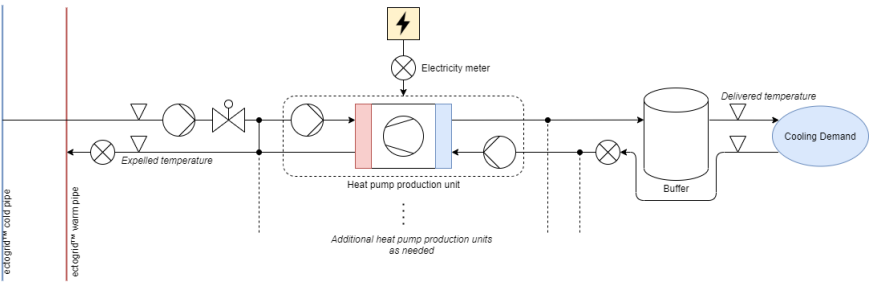

(b) An energy-sharing module providing the building with cooling

Figure 1.2: A schematic figure over a general energy-sharing module used to supply building with heat and cooling.

Figure 1.2 describes the structure of an energy-sharing module. The flow from ectogrid™ into one module is used to supply the heat pump/chiller with energy, this represents the left side of the heat pump in the figure. The right side represents the demand side, which provides the building with heating or cooling. The heat pump and chiller are controlled to meet the required heating or cooling demand in the

building. For this project, the focus will be on the flow control from ectogrid™ into a module. Thus, the demand side of the heat pump can be considered as a “black box” only representing an energy demand.

1.3 Description of ectocloud™

ectocloud™ is a software platform where measurement data from the network is collected. It plays a crucial role to provide analysis and control functionality for the network. The various measurement signals that can be extracted are: grid temperatures, control signals, flow, power, and information about compressor status. It also provides a visualization of the signals over time. In this master thesis signals from ectocloud™ will be frequently used. ectocloud™ also coordinates control. For example the reference temperatures on the grid are controlled by ectocloud™, based on variations on heating and cooling to maintain as high efficiency as possible.

1.4 Objective

In this thesis, the strategy of flow control into an energy-sharing module in ectogrid™ is investigated. The purpose of control is to keep the outgoing temperatures returned to the grid around the desired set-point temperature. Today, the controller is manually tuned, which is a time-consuming procedure and results in different settings for different energy-sharing modules. Therefore, there is an advantage in developing a generic method to tune controllers connected to the grid. Hence, one of the outcomes of this thesis is to suggest a tuning method for controller tuning of new energy-sharing modules.

It is of great importance to keep the temperatures around set-point since the efficiency of ectogrid™ requires the grid temperatures to lie within a specific range. Besides, ectogrid™ is a network of interconnections of several energy-sharing modules affecting each other. For example, if the outgoing temperature from one energy-sharing module varies, this will affect the performance in another unit. Further, large temperature variations have to be avoided to avoid the risk of freezing. If the freezing risk could be eliminated with good control, the set-point of outgoing temperature can be lowered to 6^{o}C. This would be beneficial since the efficiency in energy-sharing modules with chillers can be increased with a decreased inlet temperature.

The purpose of the project is to improve flow control for one energy-sharing module to match the specific energy demand, and to suggest a method to tune new buildings. To improve the control performance, tuning of the PI-controller is needed. Buildings are not available for testing to the extent required for the investigation of new strategies. Therefore, a model to simulate one energy-sharing module is developed

using Matlab Simulink® to give a representative picture of the system and its components. The scope is to develop a model of an energy-sharing module equipped with a heat pump. The studied module is placed in a building named 406. All buildings connected to the grid at Medicon Village are named with a specific number. To build the model and understand system dynamics, measurement data of control signals, flows and temperatures are extracted from ectocloud™. The model is used to build the controller by evaluating different control parameters compared to the manually tuned controller used today. The result from simulations is further used as support for testing. Testing is done in building 406 and 303. The test aims at trying the suggested tuning method as well as evaluating the controller performance. The results are used to identify limitations and possible improvements. Finally, the project results in a method for tuning new buildings. Additionally, limitations of the suggested controller and possible future outlooks are presented. The two authors worked closely together during the project, where both were involved in every part.

1.5 Outline of Report

- Chapter 2 covers an overview of an energy-sharing module and a description of the included components. The developed model and the results of the simulated model in Matlab Simulink® is presented.
- Chapter 3 includes the stated control specifications, evaluation methods and an explanation of the chosen tuning method. In this chapter, the results from the investigation of improved control are presented. Including control performance evaluation from simulation as well as from testing in real buildings.
- Chapter 4 presents the final pipeline for future tuning of buildings connected to ectogrid™. The chapter involves a discussion of the result, including advantages and limitation with the proposed tuning. Additionally, possible outlooks and future work is discussed in this chapter.

2

Modelling of an Energy-Sharing Module

Several buildings are connected to ectogrid™ through their own energy-sharing modules. These modules are supplied with heating or cooling from the hot/cold pipe of ectogrid™. Each module is either equipped with a heat pump, denoted VP, or a chiller, denoted KP, depending on heating or cooling demand in the building. The objective of the thesis is to improve the current flow control strategy for one energy-sharing module connected to ectogrid™ to match heating demand in the building. Therefore, it is necessary to understand the system dynamics of one energy-sharing module.

In this chapter the general structure of one energy-sharing module is described. This involves a description of the general characteristics of the main components included in the module (circulation pump, control valve and heat pump or a chiller). This chapter also includes a presentation of the current flow control strategy. In addition, the main disturbances and their impact on the system are described. To investigate new control strategies the energy-sharing module was simulated in Matlab Simulink®. Thus, models of the main components were developed based on basic dynamic, physical properties, and data collected from ectocloud™. Further, the simulated model was verified with measurement data extracted from ectocloud™. This thesis has focused on developing models for building 406, which consist of both a warm unit and a cold unit. Since similar results were obtained for both VP and KP, only the result of VP is presented in this chapter. The result for KP is found in Appendix B.

2.1 Overview of an Energy-Sharing Module

Each building connected to ectogrid™ is equipped with an energy-sharing module: a warm unit (VP), see Figure 2.1a and/or a cold unit (KP), see Figure 2.1b. Its main components are:

- A circulation pump denoted as P6:3 in VP and P5:4 in KP.
- A control valve denoted as SV2.
- A heat pump or chiller, depending on the supply of heating or cooling in the building.

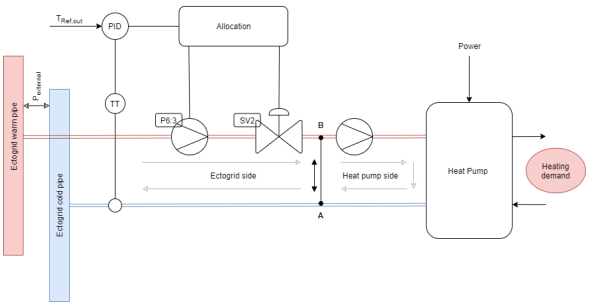

(a) Energy-sharing module equipped with a heat pump (VP).

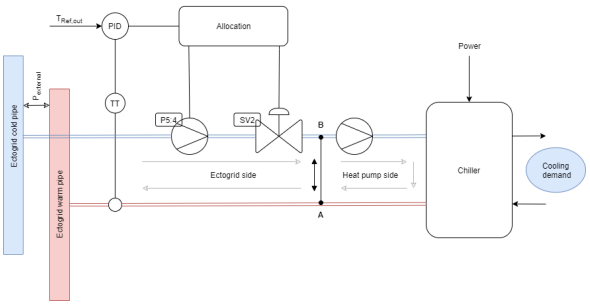

(b) Energy-sharing module equipped with a chiller (KP).

Figure 2.1: Schematic figure over an energy-sharing module equipped with a heat pump (VP) and chiller (KP) connected to the ectogrid™.

Each heat pump or chiller is equipped with a specific number of compressors stepping in and out, reflecting the energy demand in the building. The flow, therefore, needs to vary in a wide range to supply the building with the correct amount of energy. This chapter focuses on the production unit in building 406, primarily investigating the control of inlet flow altered by the circulation pump and control valve. One part of the project is to investigate how the outlet temperature is affected by the inlet flow through the circulation pump and control valve. The other part contains an investigation of how the outlet temperature is affected by other disturbances as inlet temperature, energy demand and external grid pressure.

As indicated in Figure 2.1, the system module can be divided into two separate loops:

- The outer loop denoted ectogrid™ side connected to the grid, consists of the controllable circulation pump and control valve which drives the flow from ectogrid™ into the building with a certain ingoing temperature.

- The inner loop, denoted as the heat pump side, connected to the heat pump, consists of another pump driving the water further into the heat pump and supplies the building with heating and cooling.

The two loops have different flows and are connected through a shared pipe between the warm and cold pipe, where the flow can go in both directions. The shared pipe creates two different mixing points (point A and B in Figure 2.1) depending on the flows in the two loops.

The solution of two loops is necessary since the heat pump requires a certain flow and temperature difference, which is not necessarily the same as on ectogrid™. The idea of the outer loop is to maintain a constant temperature difference between the inlet and outlet temperature by controlling the flow in the loop with the circulation pump and control valve. The inner loop agrees with the heat pump specifications and will remain with a constant flow, but with varying temperature differences. Therefore, the second pump does not affect the performance of the circulation pump connected to ectogrid™. Depending on the two flows in the different loops the mixing point can change between point A and B in Figure 2.1. When the flow of the outer loop is larger than in the inner loop, the mixing point will be in A. The mixing point will be in point B when the opposite applies. This can affect the flow, which, together with the travelled distance between the heat pump and the sensor determines the transport delay, which may affect the controller performance.

The heat transfer in the heat pump giving rise to the temperature change can be explained by a static relation presented in Equation 2.1. T_{in} is the inlet temperature to the heat pump (°C), P is the heat transfer power causing a temperature change [kW], Q is the flow [m^3/h], ρ is the fluid density [kg/m^3] and C_p the specific heat capacity for water [kJ/kgK] [*Handbook: Physical properties, correlations and equations in chemical engineering.* 2019].

$$T_{out} = T_{in} - \frac{P}{Q\rho C_p} \tag{2.1}$$

Control Strategy

Today the flow from ectogrid™ is controlled using a manually tuned PI-controller, see Figure 2.2. The flow is adjusted based on the error between the set-point temperature of outgoing temperature and actual outgoing temperature. The control signal, u from the PI-controller is further allocated to the pump, u_p and valve, u_v to adjust the flow. The resulting flow into the unit is determined by the speed of the pump causing a pressure increase equal to the overall pressure drop over the circuit. In the system, the main pressure the pump has to overcome is the pressure drop over the valve and the pressure difference between the warm and cold pipe.

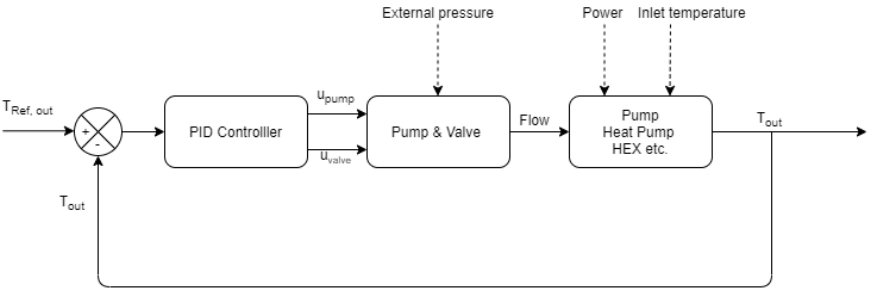

Figure 2.2: Representation of the current control structure, where external pressure, power and inlet temperature are seen as disturbances in the process.

The total control signal from the PI is allocated to the circulation pump and control valve in two different ways, either in sequence or in parallel. A sequential allocation means that the pump and valve are altered in sequence, see Figure 2.3 (left panel). With a parallel allocation the flow is altered by the pump and valve simultaneously, see Figure 2.3 (right panel). Today, the implemented control allocation varies between the buildings. When the pump and valve are controlled in sequence, the control is primarily done using the pump. It is only when the pump is running at 100% the valve is opened further, which is the case in the investigated building 406.

Disturbances

In ectogrid™ numerous disturbances in the system generate unwanted temperature fluctuations of the outgoing water returned to the grid. ectogrid™ is an interconnection of several energy-sharing modules, where changes in outgoing temperature will affect the performance of other units connected to the grid. It is important to tune the controller to reject these disturbances to maintain the outgoing temperature at the set-point. Three main disturbances are affecting the outgoing temperature; the inlet temperature, the start and stop of compressors and external pressure variations.

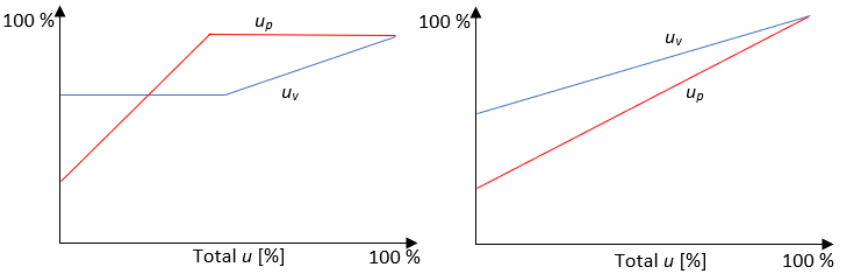

Figure 2.3: The figure shows the difference between the two allocation methods. Left panel is a sequential allocation and right panel a parallel allocation. The allocation strategy is received from E.ON.

Inlet Temperature When the temperature on ectogrid™ varies, the inlet temperature into each building will vary. This will have a direct impact on the outgoing temperature. The impact of inlet temperature on the outlet temperature can be seen in Equation 2.1. If all other parameters in the relation are held constant, a decreased inlet temperature results in a decreased outgoing temperature returned to the grid. The impact of inlet temperature can be seen in Figure 2.4. The inlet temperature to each energy-sharing module is currently measured with a high resolution reliable for control purposes.

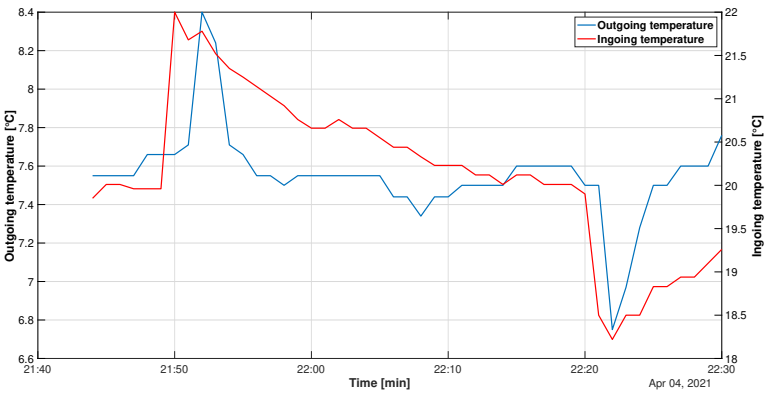

Figure 2.4: Disturbance of inlet temperature affecting the outlet temperature in building 406 VP. Data extracted from 2021-04-04.

Compressors Steps To meet the energy demand in a building, the number of compressors in the heat pumps or chillers is altered (starting or stopping). The start and stop of the compressors result in a fast increase or decrease in outlet temperature. The system is primarily sensitive to temperature drops caused by a compressor start. This is due to the risk of freezing in the system if the temperature goes below 4.5°C. Figure 2.5 shows these unwanted temperature peaks. Today there is no measured signal representing the start and stop of compressors with a resolution high enough that could be used for control purposes.

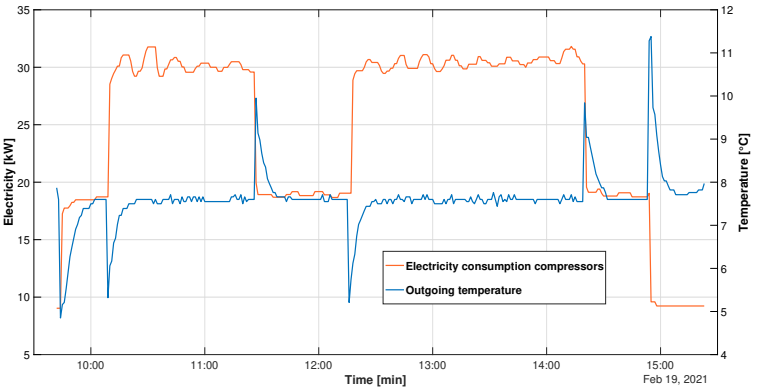

Figure 2.5: Disturbance of compressor steps affecting outlet temperature returned to grid in building 406 VP. Data extracted from 2021-02-19.

External Pressure The external pressure of the grid can be described as the differential pressure between the warm and cold pipe, $P_{external}$. Changes in the external pressure occur due to changes in heating and cooling demand in buildings connected to the grid. With varying energy demand, the grid flow is altered. This causes variations in pressure between the cold and hot pipe. In each building, the pump has to overcome pressure differences between the warm and cold pipe. When the external pressure varies, the pressure over the pump automatically changes which will affect the flow even if both pump and valve are constant, causing flow fluctuations. Today the external pressure is not measured with an accuracy high enough to use for system modelling nor as a signal for control purposes.

Dead Time

The dead time in the studied module consists of two different contributions; physical transport delays and measurement delays.

Physical transport delay Physical transport of water through the pipes between the heat pump and the temperature sensors give rise to transport delay in the system.

It is of great importance that the controller is designed considering the dead time to avoid problems with oscillations and instability [Åström and Hägglund, 1995]. Therefore, this transport delay must be determined to tune the controller accordingly.

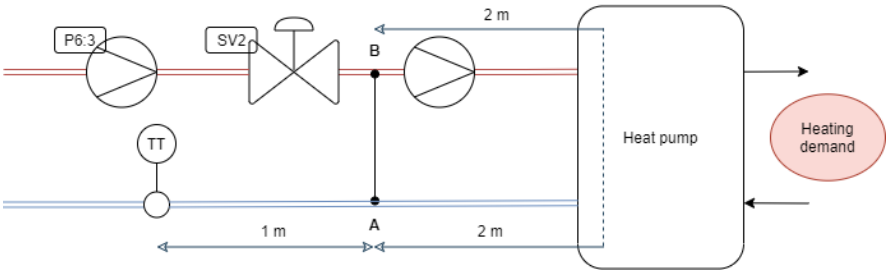

Figure 2.6: Estimated distances in building 406 VP for dead time calculations.

Figure 2.7: Photograph of building 406 VP for estimation of distances.

The travelled distance depends on whether the mixing point is located in point A or B, see Figure 2.6. The mixing point is based on the flow rates of the two loops. In the inner loop, the flow is considered constant. From technical drawings of VP in building 406 the flow of the inner loop is determined to 15 m^3/h. The maximal flow

of the outer loop is 10 m^3/h. Therefore, the flow is always larger in the inner loop compared to the outer loop. This implies that the mixing point is always located in B. Due to this observation, the dead time for the transport of water through the pipes can be divided into two parts. One part with a constant flow and one with a varying flow. The first part is the time for the water to move from mixing point B through the heat pump to point A, which is determined by the constant flow of the inner loop and pipe dimensions. Due to fast transport, the time through the heat pump is neglected. The second part is the time for the water to travel from mixing point A to the temperature sensor (TT), which is decided by the varying flow on the outer loop and pipe dimensions. See Figure 2.6 and Figure 2.7 for an overview of transport delay.

To estimate the physical transport delay some approximations and simplifications are made. The idea is to estimate the dead time from simple calculations of flows, pipe diameters and distances. The pipe diameter and the distances in the building is approximated from technical drawings and photos, see Figure 2.6. Equation 2.2 is used to calculate the cross-sectional area of the pipe. Equation 2.3 is used to calculate the velocity in the pipe and finally, Equation 2.4 is used to calculate the transport delay Dt. Where d is the pipe diameter [m], Q is the flow [m^3/s], A_c the cross-sectional area [m^2], s the pipe distance [m] and v velocity [m/s]. The estimated dead time for the two parts and the overall transport delay for VP are presented in Table 2.1. The dead time can vary between 7 and 10 seconds between the highest and lowest flow. For simulations of the system, as a simplification the dead time are held constant with a time of 8 s.

$$A_C = (\frac{d}{2})^2 \pi \tag{2.2}$$

$$v = \frac{Q}{A_C} \tag{2.3}$$

$$D_t = \frac{s}{v} \tag{2.4}$$

Table 2.1: Estimated dead time for maximum and minimum flow.

VP			
Flow [m^3/h]	Time A to TT [s]	Time B to A [s]	Total time [s]
3.7	4.8	4.8	9.6
10	1.8	4.8	6.6

Measurement delay The other contribution to the overall dead time is the measurement delay in temperature sensors. The installed temperature sensors measuring

the outlet temperature have large time constants depending on the type of sensor. This was discovered very late in the project. Therefore, it is not considered when developing the model of the unit. This is discussed further in section section 3.5.

2.2 Actuator Characteristics and Allocation Strategy

Pump Characteristics

The flow of ectogrid™ is not driven by a large circulation pump. Instead, each unit is equipped with a smaller centrifugal pump. The pump creates a differential pressure causing the water to flow into the heating or cooling unit. Thus, the purpose of the pump is both to keep up a flow on the whole grid and to provide each unit with a certain flow to meet heating or cooling demand in the building. The actual flow created by the pump is determined by the pump characteristic, describing the relationship between pressure rise and flow for different pump speed. Normally, a pump curve is used to express these relations and this differs for different pumps depending on design and size.

The pressure rise caused by the pump has to overcome pressure drops through pipes, heat pumps and across valves and other equipment in the circuit. This is called the system characteristics which shows the relation between flow and pressure drop. The characteristics of the pump and system results in a certain operating point, meaning that the generated flow through the pump gives a pressure drop over the system equal to the differential pressure over the pump, see Figure 2.8 [Trüschel, 2002].

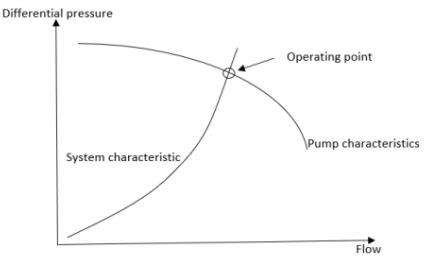

Figure 2.8: Pump and system curve resulting in a operation point depending on flow and differential pressure. Figure adapted from [Trüschel, 2002].

Regarding ectogrid™ it is mainly the pressure drop across the valve and the external pressure contributing to the system characteristics affecting the operating point in the system. The pressure in the system the pump has to overcome can be expressed

according to equation 2.5, where P_{pump} is the pressure drop over the pump, P_{valve} is the pressure over the valve and $P_{external}$ the external pressure of the grid.

$$P_{pump} = P_{valve} + P_{external} \tag{2.5}$$

The operating point changes if anything in the system changes, for example with changes in the opening of the valve or changes in external pressure of the grid. This generates a new flow according to Figure 2.9a [Trüschel, 2002]. In ectogrid™ the circulation pump used to control the inlet flow is a centrifugal pump which is controlled by its speed. An increase in speed causes an increase in flow rate. When introducing a change in speed while keeping the rest of the system constant, the operation point will change along the system curve in Figure 2.9b [Trüschel, 2002].

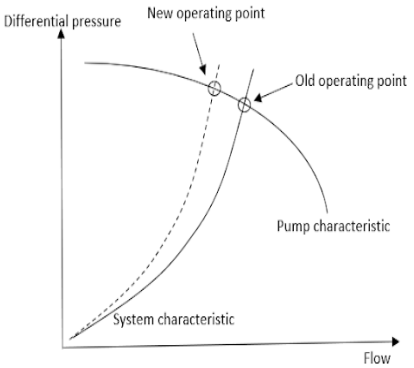

(a) Change of pump speed.

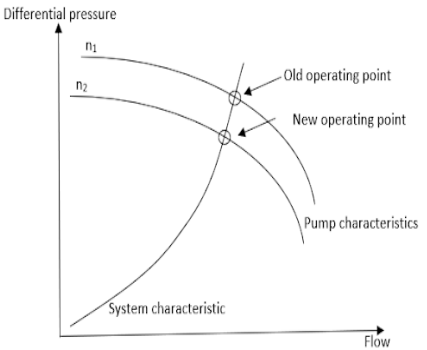

(b) Change of system characteristics.

Figure 2.9: New operating point with a system change with a change of system characteristics and a change in pump speed. Figures adapted from [Trüschel, 2002].

Valve Characteristics

In ectogrid™ control valves are mainly being used to regulate the flow outside the working region of the pump. This applies when the allocation is in sequence. Control valves can be used to regulate a flow by changing its opening thanks to an electrical actuator. The flow through a control valve can be described by Equation 2.6, where k_v is the valve capacity coefficient, ΔP, pressure drop over the valve, f(x) valve characteristics with x as the position of the valve and ρ, the density of the fluid [Hägglund, 2019a]. The valve capacity coefficient k_v can be expressed as Equation 2.7, where Q is the flow through the valve and ΔP, pressure drop across the valve.

$$Q_{valve} = k_v f(x) \sqrt{\frac{\Delta P}{\rho}} \tag{2.6}$$

$$k_v = Q_{valve} \sqrt{\Delta P} \tag{2.7}$$

The relationship between the valve opening [0-100%] and capacity of the valve k_v [m^3/h] is called the valve characteristic. The valve characteristics depend on the mechanical design of the valve and the behaviour varies between valves. Various types of mechanical valve characteristics are for example linear, equal percentage and quick opening. If the flow capacity increases as a linear behaviour with the valve opening the valve have linear characteristics and if the flow increases exponentially with valve opening the valve has equal percentage characteristics. The different types of mechanical valve characteristics are presented in Figure 2.10 [Hägglund, 2019a] [Trüschel, 2002].

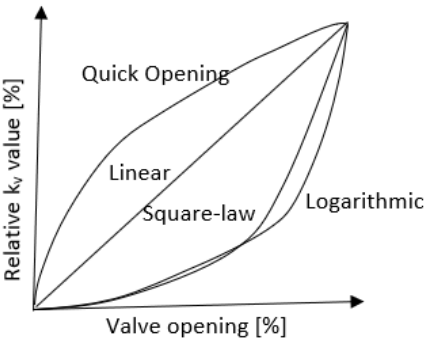

Figure 2.10: Mechanical valve characteristics presenting a linear, square-law, quick opening and logarithmic valve. Figure adapted from [Hägglund, 2019a].

The relationship between the valve opening and the flow over the valve is called true valve characteristics. This is a result of several different features depending on the type of valve and dimensions. It is the true valve characteristics that indicate how the flow is affected by the valve and how it will operate in the system [Trüschel, 2002]. When it comes to ectogrid™ the pressure drop across the valve will affect the system curve, which will alter the flow, the relationship is described in equation Equation 2.5

Pump & Valve Cooperation

There is a possibility to control the flow with the pump and valve in parallel, see Figure 2.3. In this case, the dynamics are more complicated. Looking at the pump- and system characteristics in Figure 2.9, a simultaneous change in the valve and pump will make the operating point move within an area. In addition, if the external pressure varies the system curve moves even more. To get a better understanding of the dynamics between the pump and valve in parallel 3D-plots of actual flow and control signals for pump and valve are made for VP, see Figure 2.11. The 3D-plots did not show trends good enough to draw a conclusion from it, since there are still other parameters that can affect the dynamics which are unknown. Due to this unknown dynamic behaviour of the pump and valve in parallel, it is hard to develop a model describing the flow change based on the physical characteristics. Hence, the performance of control in parallel cannot be simulated. Therefore, in this master thesis, the pump and valve work in sequence exclusively. This implies that the investigation of the impact from the allocation in terms of economics and performance is limited. To be able to compare the benefits of a sequential and parallel allocation a deeper understanding of how the pump and valve affect each other is needed.

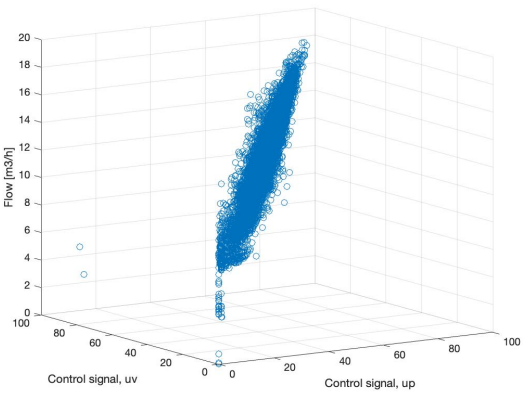

Figure 2.11: 3D-plot of control signal of pump and valve and flow.

Allocation of Pump and Valve

To maintain good control performances, the control allocation between the pump and valve has to be chosen to guarantee a wide range of flow. It is especially important to consider the limits of the flow. For example, if the heating demand in the building is low this corresponds to a low supply of heat from ectogrid™. The lowest setting of the pump speed and valve opening has to agree with the flow needed to reach the set-point temperature of 7.5°C. During the project, it was discovered that

the implemented control allocation in building 406 VP, resulted in a too high minimum flow. This was a limiting factor for reaching the desired outlet temperature. Due to this observation, the minimum valve opening was altered from 70% to 62% to be able to obtain a lower flow. This was obtained by manually adjusting the valve opening until the desired set-point temperature was reached. This change made it possible to reach the set-point temperature when the heating demand was low. Considering disturbances of inlet temperature and external pressure it is favourable if there is some space to adjust the flow even in regions where the flow is very low.

Choosing the allocation is crucial, considering economic aspects as well as the performance. Normally, it is more economically favourable to keep the valve opening large to avoid that the pump works towards higher pressure [Hägglund, 2019a]. A higher pressure increase over the pump corresponds to higher operation costs, since the power consumption, W increases with an increased speed, n. This relation is described with one of the Affinity law's Equation 2.8 [Forslund and Forslund, 2016].

$$(\frac{n_1}{n_2})^3 = \frac{W_1}{W_2} \tag{2.8}$$

2.3 Circulation Pump

Pump Model

The characteristic and physical relations of a centrifugal pump are described in the previous section. This is normally the way to describe the dynamics of a pump. This requires deep knowledge of the system characteristics in different operating points. Due to lack of system information, i.e., no measurement of the external grid pressure, the flow control by the pump are identified from measurement data. Data from ectocloud™ of flow and control signal of the pump is collected for periods when the valve has been at the constant opening. Measurement data is chosen to capture both the lower and higher working range of the pump in the interval between 30 and 100%. To find the relationship between pump speed and flow, the flow is plotted as a function of the control signal. This results in a linear behaviour between the control signal and flow. Based on the curve the slope are obtained using a linear fitting, resulting in the linear equation for lower regions of the control signal, $Q = 0.089u_p$ and for higher regions of the control signal $Q = 0.062u_p$ for VP, see Figure 2.12.

Linear behaviour between the control signal of the pump gives the proportional relation, K_p , between the control signal and flow. For lower regions in the control signal, small deviations from the linear relationship are observed. This could be expected from the theoretical pump curve, where the slope of the system curve decreases for low pump speed (Figure 2.9b). Yet, it is reasonable to assume that

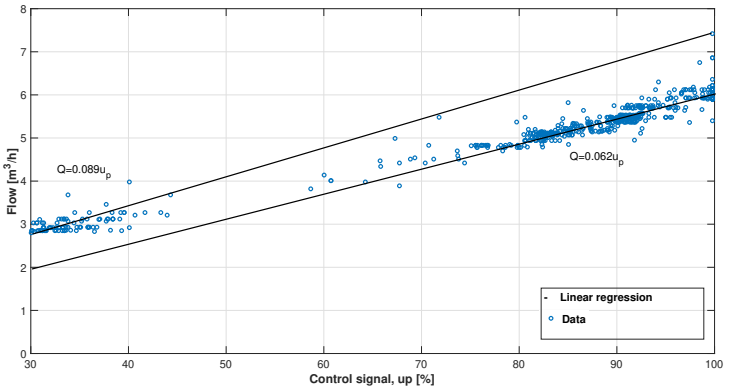

Figure 2.12: Control signal for the pump as a function of flow with linear regression $Q = 0.089u_p$ for lower regions and $Q = 0.062u_p$ for higher regions of control signal. Data extracted from 2021-02-20 to 2020-02-21.

the gain is constant in linear regions. See Table 2.2 for the resulting K_p for different regions of u_p.

Table 2.2: Resulting pump gain, K_p in different regions of the control signal.

VP	
K_p	u_p
0.089	$u_p < 0.45$
0.062	$u_p > 0.45$

Considering that the flow change is not instantaneous, the dynamics of the pump has to be taken into account. Thus, a time constant, T_p, corresponding to the time for the pump wheel to accelerate the fluid is introduced, the time constant for a pump is according to centrifugal pump simulations, in theory, less than one second [Goppelt et al., 2018][Hieninger et al., 2021]. This results in a first-order system, see Equation 2.9 [Björkman, 2006]. The Laplace transform gives the transfer function in Equation 2.10 for the pump.

$$\frac{dQ_p}{dt} = \frac{K_p u_p - Q_p}{T_p} \tag{2.9}$$

$$G_p(s) = \frac{K_p}{1 + T_p s} \tag{2.10}$$

Simulation Results of Pump

The transfer function in Equation 2.10 is used as a model for the pump in simulations. The pump gain K_p, is set according to Table 2.2 and the time constant, T_p to 0.1 min. The accuracy of the time constant is limited since the sampling time of flow from data is 1 minute and the theoretical time constant is less than a second. The pump is simulated with the control signal u_p, as the input signal. The simulated flow is further compared to measured data of the flow for the same period. Extracted measurement data from ectocloud™ is chosen to capture a wide working range of the pump to make sure that the model works in a large region. In addition, data is extracted for a period when the valve has been at the constant opening.

The results of the simulation compared to data are presented in Figure 2.13. Figure 2.13a shows data over the control signal used as input and Figure 2.13b shows the simulated flow compared to data. It is observed that the simulated pump and extracted data of flow agree well, with small deviations.

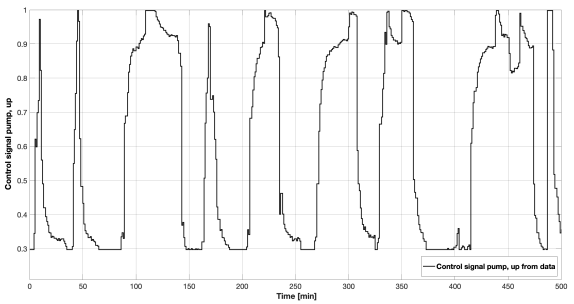

(a) Control signal of the pump from measurement data.

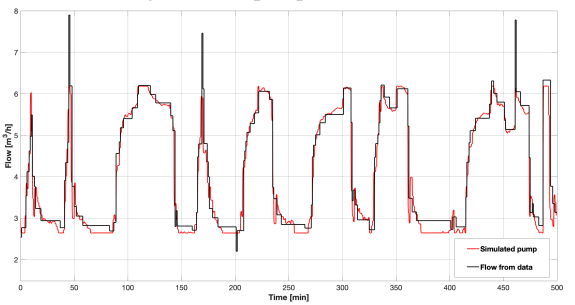

(b) Simulation results of the pump as a first order system compared to measurement data of the flow.

Figure 2.13: Measurement data of the control signal used for simulating the pump and the result of the simulated pump compared to data of the flow. Data extracted from 2021-02-17.

2.4 Control Valve

Valve Model

As described for the circulation pump, unknown system characteristics are requiring deeper knowledge to use the physical dynamics to model the valve. Therefore, data from ectocloud™ of flow and control signal of the valve is collected to investigate flow control using the valve. Since the valve has been at its minimum opening of 62 % in VP, the impact of the flow can only be investigated in the regions above. Also, due to a lack of measurement data when the valve has varied and the pump has been at a constant speed, the valve is hard to investigate. To find the relationship between valve opening and flow, the flow is plotted as a function of the control signal. This resulted in a linear behaviour between the control signal and flow but with some deviations at lower regions of the control signals. Linear fitting of the curves results in the linear equation $Q = 0.28u_v - 10.65$, see Figure 2.14.

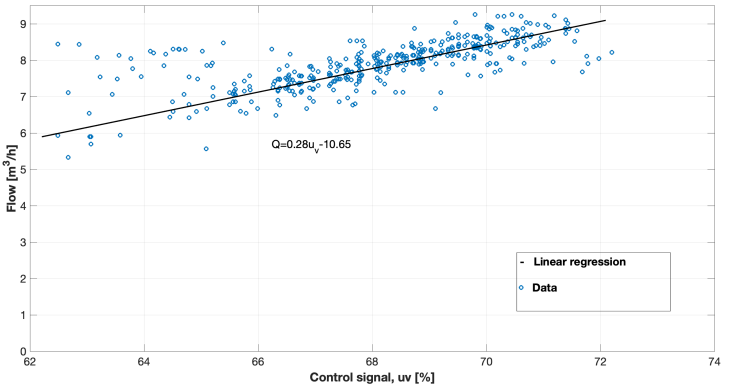

Figure 2.14: Control signal of the valve as a function of flow with linear regression $Q = 0.28u_v - 10.65$. Data extracted from 2021-02-21 to 2021-02-22.

The control signal for the valve, u_v and the flow is approximated with a suitable linear fitting. Hence, a proportional gain, K_v between the control signal and flow could be introduced. Since the time for the valve to open is not instantaneous, time dynamics are considered by introducing the time constant, T_v. The time constant describes the time for the motor to move the valve position to change the flow. According to technical descriptions of the valve, this time is between 15-60 s [*Ventilställdon M400* 2008] [*Ventilställdon M800* 2010]. Finally, the valve is modelled as a first-order system, see Equation 2.11, where Laplace transform gives the transfer function between the control signal and flow presented in Equation 2.12.

$$\frac{dQ_v}{dt} = \frac{K_v u_v - Q_v}{T_v} \tag{2.11}$$

$$G_v(s) = \frac{K_v}{1 + T_v s} \tag{2.12}$$

Simulation Result Valve

The transfer function in Equation 2.12 is used as a model for valve simulation. The valve gain K_v, are set to 0.2 based on the linear estimation and the time constant T_v, are set to 0.5 min based on the technical description of the valve. For simulations, the control signal, u_v for the valve is used as the input signal. To evaluate the model, the simulated flow is compared to measurement data of the flow. Measurement data is extracted from ectocloud™ and data is chosen to capture a large working region of the valve during a time when the pump has been at a constant speed.

The results of the simulated valve is presented in Figure 2.15, representing data over the control signal used as input and the simulated flow compared to data. The fit of the first-order system compared to data are good but with some deviation. This might be explained by deviations from the linear relation of flow and control signal.

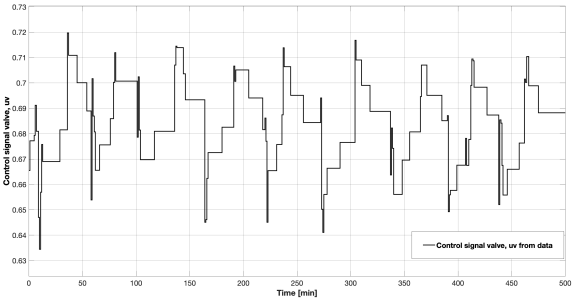

(a) Control signal of the valve from measurement data.

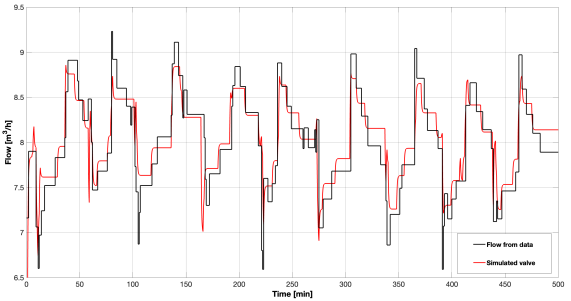

(b) Simulation result for valve as a first order system compared to measurement data for flow.

Figure 2.15: Measurement data of the control signal used for simulating the valve and the result of the simulated valve compared to data of the flow. Data extracted from 2021-02-21.

2.5 Heat Pump

Heat Pump Characteristics

In ectogrid™ heat pumps and chillers are used to supply buildings with heating and cooling. A heat pump cycle consists of four main steps and the cycle is described in figure 2.16 [Eastop and McConkey, 1993]. The liquid in the heat pump passes through an evaporator. The energy required to evaporate the liquid is supplied from the surrounding, P_1. In ectogrid™ this represents the heat supplied from the grid. The evaporated liquid is further compressed to a higher pressure. This requires energy in form of electricity, W. The power input to the compressor is important since this is the main item of running cost. After compression is the vapour condensed in a condenser, where the amount of energy revealed to the surrounding, denoted P_2. In ectogrid™, this energy is used to supply the building with heat. Regarding P_1 and P_2, the opposite applies for a chiller.

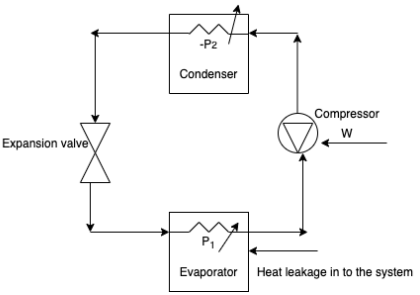

Figure 2.16: Schematic figure of the heat pump cycle presenting evaporator, condenser, compressor and expansion valve. Figure adapted from [Eastop and McConkey, 1993].

From the first law of thermodynamics, the relation of input power and heat leakage P_1 and P_2 can be expressed, see equation 2.13 [Eastop and McConkey, 1993].

$$W + P_1 = -P_2 \tag{2.13}$$

The performances of the chiller- and heat pump are evaluated by their coefficient of performance (COP), which is the same as the efficiency, see Equation 2.14 and 2.15 [Eastop and McConkey, 1993].

$$COP_{cool} = \frac{P_1}{W} \tag{2.14}$$

$$COP_{heat} = \frac{-P_2}{W} \tag{2.15}$$

Heat Pump Model

To build up a model over the heat pump the power causing the temperature change is expressed, representing P_1 in Figure 2.16 for VP. This heat transfer value can be extracted from ectocloud™ based on flow measurement, inlet and outlet temperatures. Instead of using this value of heat transfer, the electricity consumption of the heat pump can be related to the heat transfer according to Equation 2.14. Therefore, the relationship of power consumption and heat transfer power is investigated to determine COP_{cool} for the heat pump. Measurement data of the electrical consumption as well as the heat transfer of ectogrid™ is exported from ectocloud™. Furthermore, COP is estimated to approximately 4 for VP with some variations for the different compressor steps. The result of the estimated heat transfer compared to heat transfer from data are presented in Figure 2.17.

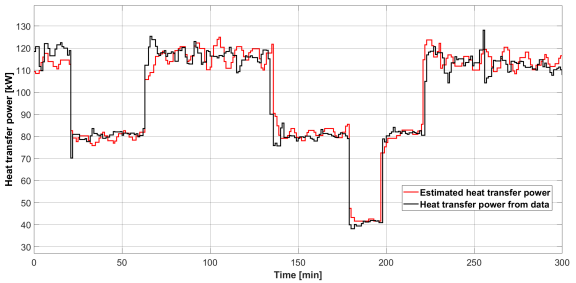

Figure 2.17: Estimated heat transfer power from COP and electrical power consumption compared to measurement data of heat transfer power. Data extracted from 2021-02-21.

The overall heat transfer causing the temperature change of the water back to ectogrid™ is described by the static relation in Equation 2.1. This was primarily used as a model for simulations. Since the change of temperature is not instantaneous the model is further developed to slow down the temperature changes in the simulations to match measurement data. In the real process, water is flowing into the system with a certain flow, Q and an inlet temperature, T_{in}, see Figure 2.18. This flow is mixed with the water coming out from the heat pump with temperature, T_{out} in point B before it enters the heat pump. To simplify this, the mixing point and the heat pump can be assumed to be a homogeneous tank of water with a specific volume, denoted τ. The volume and temperature of the tank will change with time depending on the flow, inlet temperature and power, W. The power is the electricity consumption in the heat pump reflecting the heat transfer causing temperature change of the water. The simplified model is also described in Figure 2.18. The model describing the heat pump is presented in Equation 2.16, where τ can be seen as a time constant of the heat pump, c_p specific heat capacity, COP a conversion factor between electric power and heat transfer and $\dot{T_{out}}$ is the change of outgoing temperature in time.

$$\tau \dot{T}_{out} = c_p m (T_{in} - T_{out}) - COP \cdot W \tag{2.16}$$

The heat pump model results in a nonlinear relation between flow, inlet temperature, power and outlet temperature. To investigate how the control of the system may be improved the heat pump model is linearized around an arbitrary stationary point. Linearization of Equation 2.16 around a stationary point m_0, $T_{in,0}$, $T_{out,0}$ and P_0 results in the linearized transfer function in Equation 2.17. Where m is the mass flow, T_{in} is the inlet temperature, T_{out} is the outlet temperature and P is the heat transfer power.

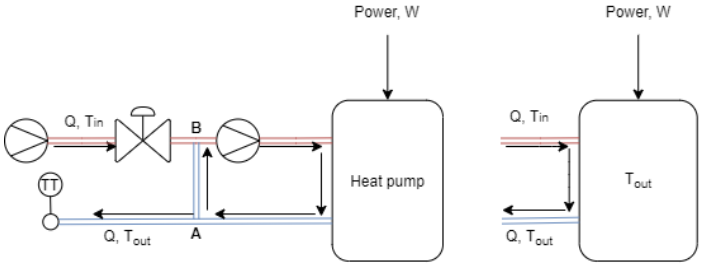

Figure 2.18: Schematic figure over the system and the simplified model used to build up the the dynamic model of the heat pump.

$$\Delta T_{out} = \frac{P_0}{C_p m^2 (1+\tau s)} \Delta m - \frac{1}{1+\tau s} \Delta T_{in} + \frac{1}{C_p m_o (1+\tau s)} \Delta P \tag{2.17}$$

The system is linearized around a stationary point representing a specific operating point. One main reason causing different operating points is the different compressor stages in the heat pump, corresponding to different stationary flows. Variations of the inlet temperature is also a reason for varying operating flow. Therefore, to reflect and simulate various scenarios occurring in reality the system is divided into different operating points. This is based on the numbers of compressors, corresponding to different levels of electricity consumption and the compatible mass flow, m. At stationarity, the inlet temperature is set to 20^{o}C since this is the desired temperature of the warm pipe. Table 2.3 presents the different operation points in VP.

Table 2.3: Operation points corresponding to compressor steps, presenting the number of compressors in operation, electricity consumption and stationary mass flow.

Operation points		
Number of compressors	Electricity consumption [kW]	Mass flow[kg/s]
1	10	0.76
2	20	1.52
3	30	2.27

Simulation Results of Heat Pump

The dynamic model of the heat pump is implemented and simulated with the inlet temperature, flow, and electricity power as input signals. Measurement data extracted from ectocloud™ are chosen to capture a large working range. Figure 2.20a, shows data for inlet temperature. Figure 2.20b shows data for the electricity consumption, reflecting one, two and three compressors. Figure 2.20c shows data for the flow. Simulated results of the heat pump is compared to measured data of the outgoing temperature, T_{out}. The result is presented in Figure 2.19. There are some deviations in the size of the temperature peaks from the simulation model compared to real data. This is probably due, the simplification of time dynamics in the heat pump model.

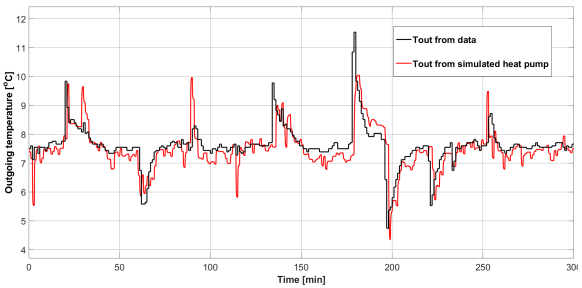

Figure 2.19: Simulated results for heat pump of outgoing temperature compared to measurement data of outgoing temperature. Data extracted from 2021-02-21.

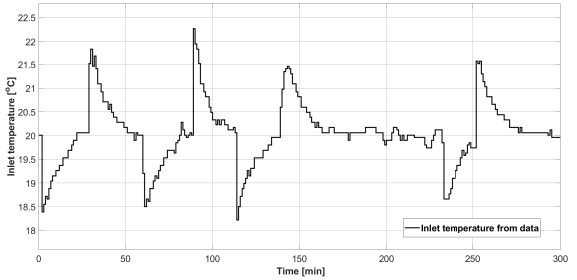

(a) Inlet temperature.

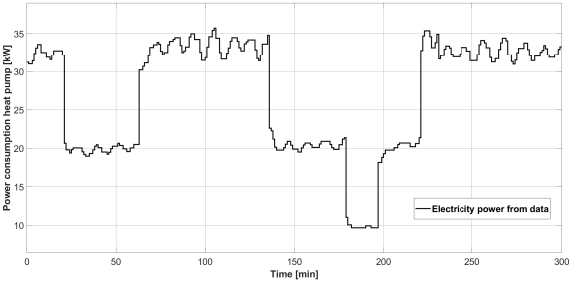

(b) Electricity consumption of compressors.

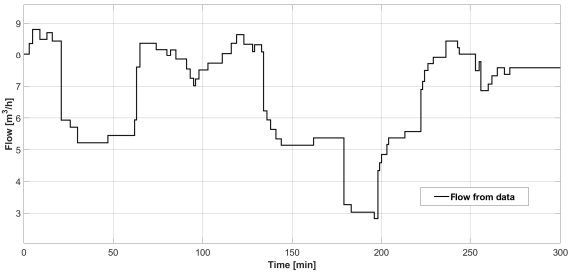

(c) Flow.

Figure 2.20: Extracted data of inlet temperature, electricity consumption of compressors and flow used in simulations of the closed loop system. Data extracted from 2021-02-21.

2.6 Closed-loop

Finally, the whole system is simulated by introducing a PI-controller in sequential form. It is assumed to keep the pump and valve separate and to use a constant dead time of 8 s representing the physical transport delay. In addition, the system is simulated in continuous time. The Simulink® model is presented in Appendix A.

A block diagram over the closed system can seen in Figure 2.21, where set-point temperature, inlet temperature and heat transfer are input signals. C(s) represents the PI-controller, A is the allocation factor, G_p(s) is the transfer function of the pump. P_1(s), P_2(s) and P_3(s) represents the linearized heat pump. Where P_1(s) is the transfer function from flow to outlet temperature, P_2(s) is the transfer function from inlet temperature to outlet temperature and P_3(s) is the transfer function from heat transfer to outlet temperature. The time delay is separated between the physical transport delay, Dt (e^{-Dts}) and measurement delay, Dm (e^{-Dms}). The resulting equation affecting the outlet temperature is presented in Equation 2.18. P_1(s), P_2(s) and P_3(s) are expressed in Equation 2.19, 2.20 and 2.21 respectively.

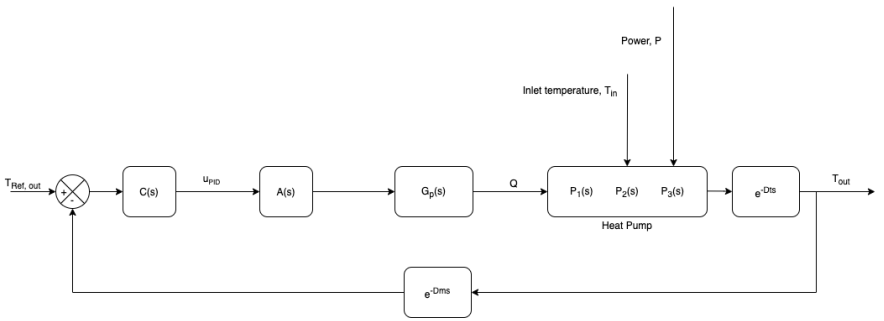

Figure 2.21: Schematic block flow diagram of control structure with the simplified linearized heat pump model. Where C(s) is the controller transfer function, A(s) a allocation factor, G_p(s) transfer function of the pump, P_1(s), P_2(s), P_3(s) transfer functions of the heat pump and including measurement delay Dm and transport delay Dt.

$$\Delta T_{out} = \frac{P_1(s)G_p(s)A(s)C(s)e^{-Dts}}{1+P_1(s)G_p(s)A(s)C(s)e^{-Dts}e^{-Dms}}\Delta T_{ref} + \frac{P_2(s)}{1+P_1(s)G_p(s)A(s)C(s)e^{-Dts}e^{-Dms}}\Delta T_{in} + \frac{P_3(s)}{1+P_1(s)G_p(s)A(s)C(s)e^{-Dts}e^{-Dms}}\Delta P \tag{2.18}$$

$$P_1(s) = \frac{P_0}{C_p m^2 (1+\tau s)} \tag{2.19}$$

$$P_2(s) = -\frac{1}{1+\tau s} \tag{2.20}$$

$$P_3(s) = \frac{1}{C_p m_o (1+\tau s)} \tag{2.21}$$

The PI-controller is simulated using Equation 2.22 with the corresponding transfer function presented in Equation 2.23. Design parameters for the PI are presented in Table 2.4 for VP. Also, the same allocation as for the real controller is introduced to allocate the control signals to the pump and valve, see Table 2.5 for VP.

$$c(t) = K(e(t) + \frac{1}{T_i}\int_o^t e(t)\,dt\ + T_d\frac{de(t)}{dt}) \tag{2.22}$$

$$C(S) = (1 + \frac{1}{T_i s} + T_d\frac{N}{1+N/s}) \tag{2.23}$$

Table 2.4: Current PID-parameters of the controller presenting the gain, K T_i, integral time [s] and T_d, derivative part.

B406 VP		
K	T_i	T_d
1/20	150	0

Table 2.5: Control signal allocation from control signal u_{PID} to u_{pump} and u_{valve}.

B406 VP		
u_{PID}	u_{Pump}	u_{valve}
$u < 0.4$	$1.75u + 0.3$	0.62
$0.4 < u < 0.45$	1	0.62
$u > 0.45$	1	$38/55u + 17/55$

Results for the simulated closed loop for VP are presented in Figure 2.22, where the simulated outgoing temperature is compared to measurement data of the outlet temperature in Figure 2.22a. Data used for simulation is the same as for heat pump simulations, see Figure 2.20. As can be seen in the results of the simulated outgoing temperature compared to measurement data, the simulated temperature drops compared to the real data. This will be considered as a limitation in the model but yet good enough for this purpose. The simulated control signals for the pump, see Figure 2.23a and valve, see Figure 2.23b, as well as the overall flow, are compared to measurement data, see Figure 2.22b. To conclude, the simulation result for the closed-loop agrees well with extracted data of temperature, flow and control signals for pump and valve. Similar results are observed for the closed-loop of KP, which is presented in Appendix B.

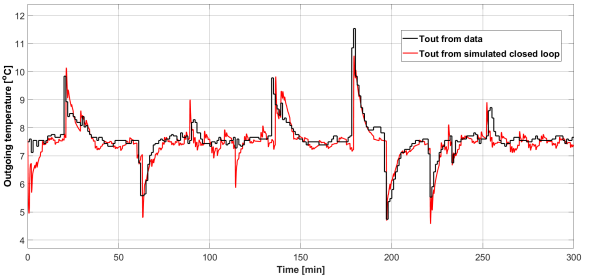

(a) Outgoing temperature compared to measurement data.

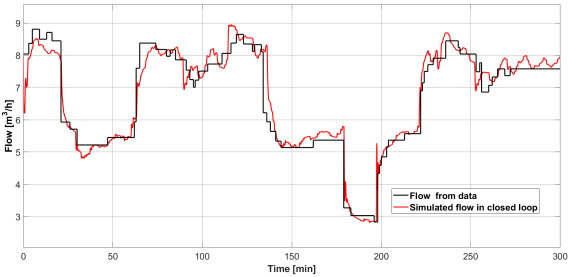

(b) Flow compared to measurement data.

Figure 2.22: Simulated results of outgoing temperature and flow for the closed loop compared to measurement data extracted from ectocloud™. Data extracted from 2021-02-21

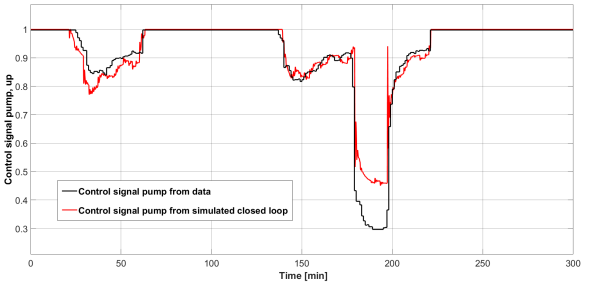

(a) Control signal of the pump compared to measurement data.

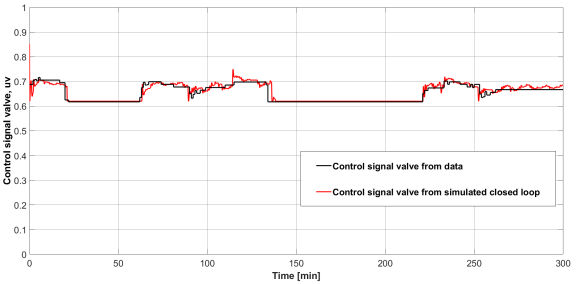

(b) Control signal of the valve compared to measurement data.

Figure 2.23: Simulated results of the control signals (pump and valve) for the closed loop compared to measurement data extracted from ectocloud™. Data extracted from 2021-02-21.

3

Flow Control of Energy-Sharing Modules

It is important to keep stable and constant temperatures on ectogrid™ to guarantee high efficiency in the heat pumps/chillers. This requires an efficient flow control into each energy-sharing module to maintain the desired outgoing temperature back to the grid. This chapter focus on finding a proper tuning of the PI-controller as introduced in the previous chapter.

First, the control specifications are formulated and evaluated. Performances, including disturbance rejection, are investigated and evaluated according to an evaluation method described in this chapter. To tune the controller properly an analytical investigation of the design parameters in the PI is carried out. This is used as a base for suggesting the final tuning method for new buildings connected to the grid. Mainly VP in building 406 is investigated using the simulated model of one energy-sharing module. Real testing on building 303 is performed to evaluate the performance of the tuning method.

3.1 Control Specifications

Specifications are stated to evaluate the performance of the controller. The main objective of the controller is to maintain the outlet temperature around a set-point of 7.5°C while preserving stability. This is extra important since ectogrid™ is an interconnection of many energy-sharing modules and oscillations can easily be propagated and amplified. The controller needs to be robust because of a wide range of operating points and non-linearities in the system.

One objective is to reduce the temperature-peak appearing when a compressor is started or stopped. It is especially important that the temperature does not dip below 4.5°C due to freezing risk in the heat exchangers in the heat pumps. If the temperature goes below 4.5°C a freezing alarm is turned on, which causes the heat pump

to stop. This is primarily a risk in VP when one compressor is started. The large increase in heat transfer causes a fast drop in outgoing temperature. If these peaks could be reduced the set-point temperature could be lowered. This would be beneficial for several parts of ectogrid™ since it will i.e. increase efficiency in buildings equipped with a chiller with a lowered grid temperature.

The designed controller should also reject disturbances caused by inlet temperature. This is important since if the outlet temperature from one module oscillates this will affect the inlet temperature in the next building. The last specification is to find a control strategy that is robust against variations in external pressure. If the external pressure varies this will cause fluctuations of the flow into an energy-sharing module. A change in flow will result in a changed outgoing temperature, causing disturbances in inlet temperature in the next module.

3.2 Performance Evaluation Methods

The PI-parameters is evaluated from different aspects using the simulation model described in chapter 2 as a pre-study. After evaluation of controller performance using simulations, the design of the controller is tried on a real building. The two different evaluation methods are described in this section.

Evaluation using Simulation

Experiments can be performed using the simulation model of an energy-sharing module to get an idea of a suitable tuning method. It can be hard to do an experiment for every new building, therefore the simulations are used as a first indication. According to the stated specifications, different scenarios are developed to assess control performance. Therefore, step changes are introduced to capture the effect of different disturbances.

- Steps of inlet temperature varying between 18°C and 20°C, see Figure 3.1. Introduced to evaluate controller performance when inlet temperature varies. Simulated with constant heat transfer power corresponding to two compressors in operation.

- Steps of compressors moving from one, two and three reflecting varying heating/cooling demand in buildings, see Figure 3.2. Introduced to evaluate the controller performance when compressors start and stop. Simulated with a constant inlet temperature of 20°C.

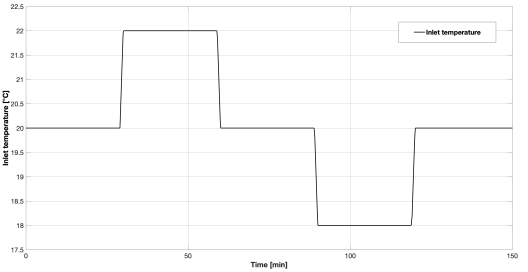

Figure 3.1: Inlet temperature steps reflecting when inlet varies on the grid.

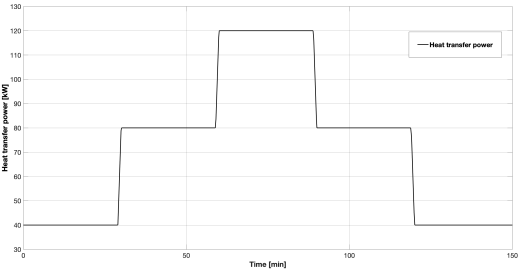

Figure 3.2: Heat transfer power steps reflecting number of compressors in operation.

- Steps of flow reflecting varying external grid pressure, see Figure 3.3. Introduced to evaluate controller performance with varying external pressure causing fluctuations of the flow. Simulated with a constant inlet temperature of 20°C and heat transfer power corresponding to two compressors in operation.

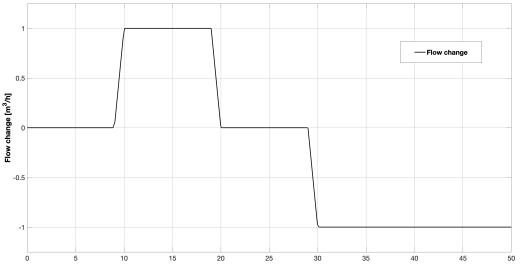

Figure 3.3: Flow change reflecting varying external pressure on the grid.

- Finally, to capture the behaviour of both variations of inlet temperature, start and stop of compressors and external pressure, data is extracted from

ectocloud™ according to Figure 2.20. This is used to evaluate the controller performance when several disturbances appear simultaneously.

Evaluation in a Real Building

The resulting PI-design from the pre-study is further tested in a real building. The performance of the design is mainly evaluating:

- The peak in outgoing temperature when a compressor is starting.
- The stability in the system considering oscillations in outgoing temperature.

3.3 Controller Tuning

In this section, the PI-controller in building 406 is tuned and the corresponding results are compared with the current PI (manually tuned). The objective is to be able to reproduce this control synthesis for new buildings connected to the grid. Therefore, different tuning methods are investigated to find a suitable one for this process, which could be easily adapted to new systems.

The normalized time delay, τ determines how complicated it is to control a system. It is defined as:

$$\tau = D/(D+T) \tag{3.1}$$

Where D is the dead time and T the time constant of the process. This relation can be used to characterize process dynamics and it indicates how hard the system is to control. Generally, with a smaller τ of the process, it results in an easier system to control. With an increase of τ the difficulty in controlling the system increases. A small τ is called lag-dominated processes and with a τ close to one it is called delay-dominated processes [Åström and Hägglund, 1995]. Some reasonable limits for τ are for lag-dominated $0<\tau<0.2$, for balanced processes $0.2<\tau<0.6$ and for delay-dominated processes $0.6<\tau<1$ [Hägglund, 2019b].

The normalized time-delay for an energy-sharing module (as modelled in chapter 2) is equal to 0.32, with a time delay, D= 10 s and time constant, T=20 s (based on step response with simulations see section 3.4) which indicates that the process is balanced and easy to control.

Lambda-tuning Method

Different tuning methods have been considered in this project to design the PI-controller for ectogrid™'s energy-sharing modules:

- Ziegler-Nichols tuning method [Åström and Hägglund, 1995]

- Cohen-Coon tuning method [Yu and SpringerLink (Online, 2006]
- Haalman tuning method [Åström and Hägglund, 1995]
- Pole-placement [Åström and Hägglund, 1995]
- One-third rule [Hägglund, 2019b]
- Lambda-tuning method [Åström and Hägglund, 1995]

Out of the tuning methods presented above, the lambda-tuning method is today one of the most commonly used tuning methods in the industry. The method was developed for dead time processes and hence a good option for tuning the controller in ectogrid™. The lambda-tuning method yields a relatively simple way to calculate controller parameters and with λ as a tuning parameter. It adds a dimension to adjust the parameter depending on the desired robustness [Åström and Hägglund, 1995]. Therefore, the lambda-tuning method is picked as a tuning method as it is a commonly used method and easy to implement on new buildings. Lambda-tuning is based on pole-placement relating to the closed-loop time constant. For a first-order system with time delay and a PI-controller, using $T_i = T$, the transfer function becomes [Panagopoulos et al., 1997]:

$$P(s)C(s) = \frac{KpK}{1 + sT_{cl}} e^{-Ds} \tag{3.2}$$

Further, using Taylor series approximation of the time delay an approximation of the closed-loop time constant, λ, can be introduced. The PI-parameters can further be calculated with Equation 3.3 and Equation 3.4 [Panagopoulos et al., 1997].

$$K = \frac{1}{K_p} \frac{T}{\lambda + D} \tag{3.3}$$

$$Ti = T \tag{3.4}$$

According to lambda-tuning method, the tuning parameters can be determined from a step response experiment of the open-loop process. Thanks to simple formulas the PI-parameters can be calculated, see Equation 3.3 and 3.4. As explained in [Åström and Hägglund, 1995], lambda tuning consists of the following steps:

- From the step response, see Figure 3.4, read the dead time, D, the time constant of the process, T and calculate the static gain, $K_p = \frac{\Delta y}{\Delta u}$.

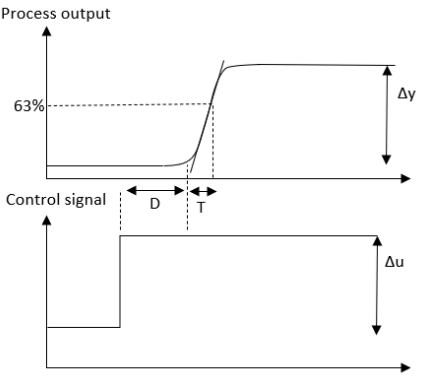

Figure 3.4: Step response for the process for the Lambda method. Figure adapted from [Åström and Hägglund, 1995].

- Choose the desired closed loop time constant for the system, λ. A common choice is to relate the desired closed loop time constant to the system and to make the choice $\lambda = T$. If more robustness is desired make the choice $\lambda = 2T$.
- Calculate the PI-parameters K and T_i for the controller according to Equation 3.3 and Equation 3.4.

3.4 Pre-study using Simulations

The simulated model is used for pre-studies according to section 3.2. In this section, a pre-study using the lambda-tuning method is presented.

According to lambda-tuning method, the tuning parameters are based on step response experiment. Due to nonlinearities in the system, the controller design varies depending on which operating point the system is tuned at. It is therefore decided to tune the controller for the worst case. The worst case corresponds to the case of the highest static gain, which requires the lowest controller gain [Åström and Hägglund, 1995]. The different operating points in the system depends mainly on the number of compressors in operation and inlet temperature, see Table 2.3.

The resulting static gains are similar for the three different operating points. Instead, it is the dead time being the limiting factor for tuning. A long dead time results in a less stable system. The longest dead time appears at the lowest flow; when the time for physical transport of water is the longest. Thus, the physical transport delay of 10 s is used. A step change of 0 to 0.17 in the control signal is introduced. The

result of the step response for one compressor is presented in Figure 3.5. The time constant, T is identified to 18 s. The static gain, Kp is calculated to 19.4 and dead time, D to 10 s. According to Equation 3.3 and Equation 3.4, using λ=T it results in K=1/29 and T_i=20s.

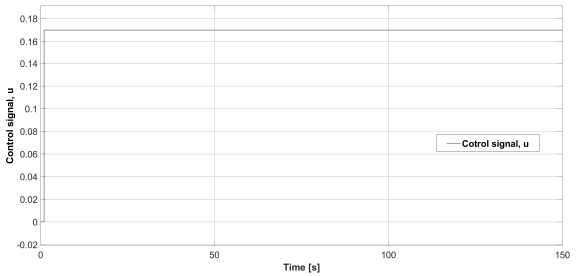

(a) Control signal.

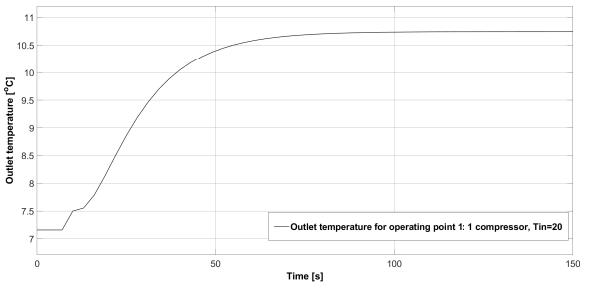

(b) Process output.

Figure 3.5: Simulated step response experiment for VP in building 406.

The controller is evaluated and compared to the performance of the current manually tuned PI-controller. The result, including outgoing temperature and control signal for the different cases, are presented below in Figure 3.6-3.9. The ability to reject disturbances from compressor steps is presented in Figure 3.6, disturbances in inlet temperature in Figure 3.7 and flow fluctuations in Figure 3.8. Finally, the results using real data of inlet temperature and electricity consumption is presented in Figure 3.9. From simulations, it is concluded that the new design results in lower peaks and faster settling time in all scenarios. But, the temperature overshoot before settling. Especially in the case when the inlet temperature varies from 20-18^{o}C and with a compressor step between two and three compressors.

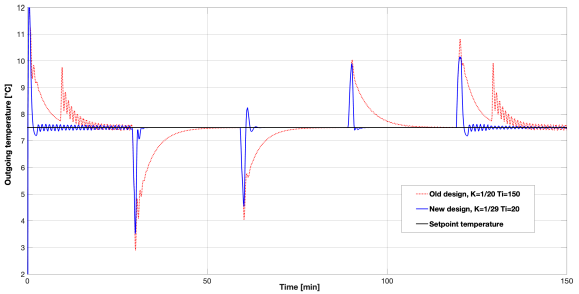

(a) The resulting outgoing temperature of the new designed PI compared to the manually tuned PI.

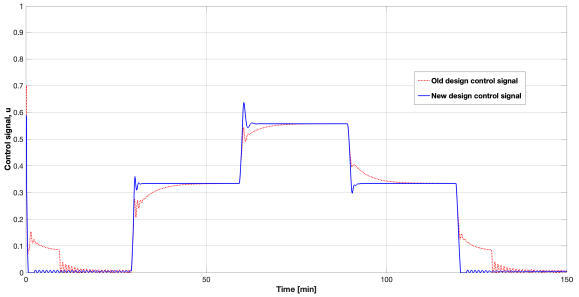

(b) The control signal of the new designed PI compared to the manually tuned PI.

Figure 3.6: Simulated controller performance for the manually tuned PI compared to the new design of the PI when introducing a compressor step.

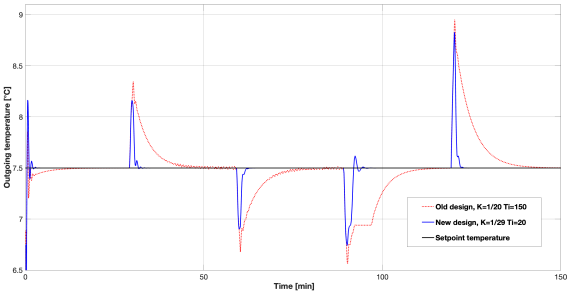

(a) The resulting outgoing temperature of the new designed PI compared to the manually tuned PI.

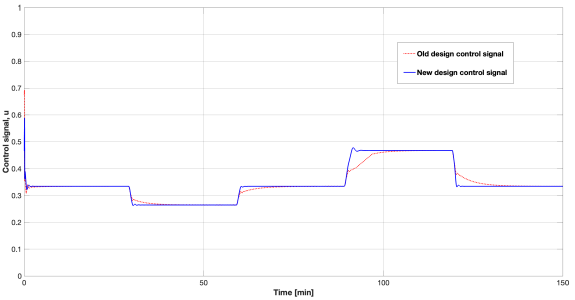

(b) The control signal of the new designed PI compared to the manually tuned PI.

Figure 3.7: Simulated controller performance for the manually tuned PI compared to the new design of the PI when introducing a step in inlet temperature.

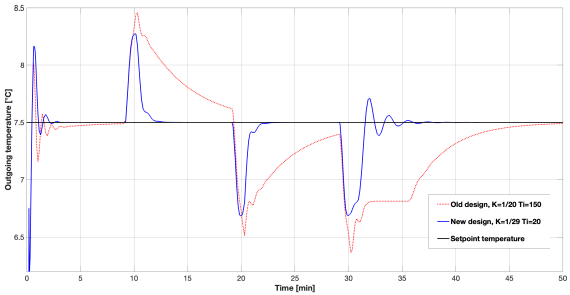

(a) The resulting outgoing temperature of the new designed PI compared to the manually tuned PI.

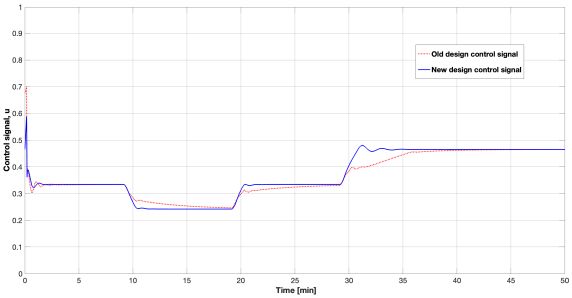

(b) The control signal of the new designed PI compared to the manually tuned PI.

Figure 3.8: Simulated controller performance for the manually tuned PI compared to the new design of the PI when introducing flow fluctuations.

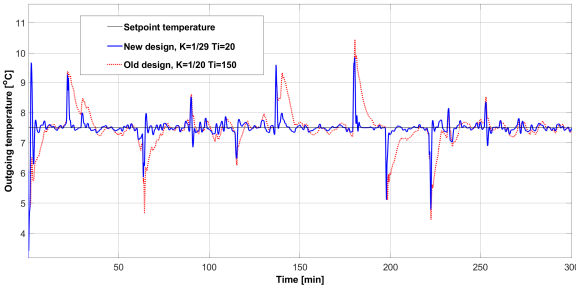

(a) The resulting outgoing temperature of the new designed PI compared to the manually tuned PI.

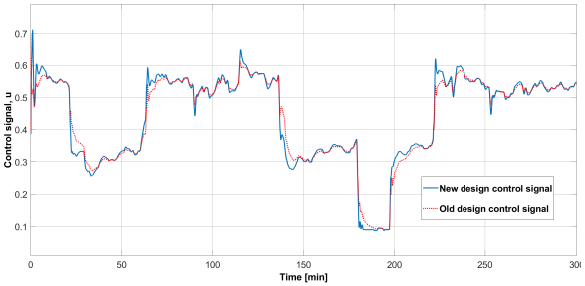

(b) The control signal of the new designed PI compared to the manually tuned PI.

Figure 3.9: Simulated controller performance for the manually tuned PI compared to the new design of the PI when introducing real data of inlet temperature and heat pump power.

One feature of using lambda-tuning is that the λ-parameter can be adjusted to increase or decrease the controller gain, K depending on desired robustness. According to theory, a common choice is λ equal the time constant, T of the system. To increase the robustness of the system λ can be set equal to $2T$ instead [Åström and Hägglund, 1995]. To understand the impact of λ, simulations of the system with different values of λ is performed, see Figure 3.10. The choice of λ=2T, corresponding to a lower gain, results in less oscillations but higher temperature peaks. A decreased λ of λ=0.5T, corresponding to a higher controller gain, results in lower temperature peaks but more oscillations. Thus, it was chosen to keep λ=T. The simulated results in the pre-study motivate to try this configuration of parameters in reality.

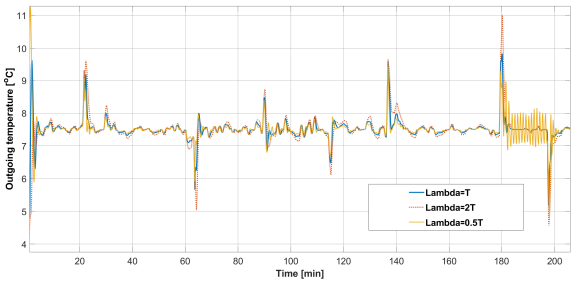

(a) Outgoing temperatures

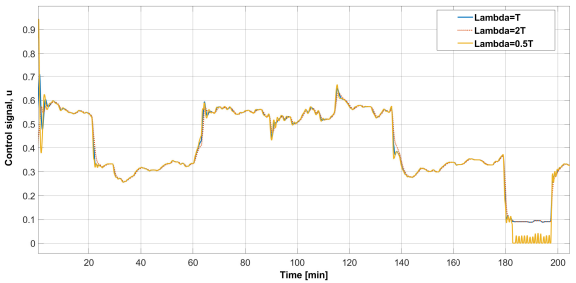

(b) Control signals

Figure 3.10: Investigation of the controller performance for different values of λ using simulations.

3.5 Testing Control Performance in Building 303

In this section, the proposed design technique is tested on a building. Unfortunately, the studied building 406, was out of operation in a couple of weeks coinciding with the time for testing. Therefore, a similar building 303, also equipped with a heat pump (VP) and a chiller (KP) unit was used for testing. First, a model of the energy-sharing module in the building is developed, in the same way as described in chapter 2. This is used to compare the simulated step response with the real step. The manually-tuned PI controller in this building is given by K=1/20 and T_i=150s. The test included the following:

- A step response experiment to compare the simulated model with the real energy-sharing module.
- Calculations of new design parameters of K and T_i according to Lambda-method using λ=T.
- Implementation and evaluation of new design in terms of peak height in outgoing temperature related to compressor step and oscillations.

A step was performed with one compressor in operation allowing to determine the characteristics of this module: dead time $D = 24$ s, a time constant $T = 18$ s and static gain $Kp = 6.4$. The real step response is compared to the simulated one to verify the dynamics in the system ($Kp = 10$, $T = 19$, $D = 5$s), see Figure 3.11. The introduced step is presented in Figure 3.12. The time constant is similar to the one received from simulations. The main difference between the step responses is the long dead time. The theoretical transport delay is calculated in the same way as described in section 2.1, to a dead time of 5 s. New parameters based on the lambda-tuning method is calculated based on the step response resulting in a K=1/15 and T_i=18s, compared to the manually tuned parameters of K=1/20 and T_i=150s. The new design parameters are evaluated on the process based on temperature peaks from a compressor step and oscillations in the system.

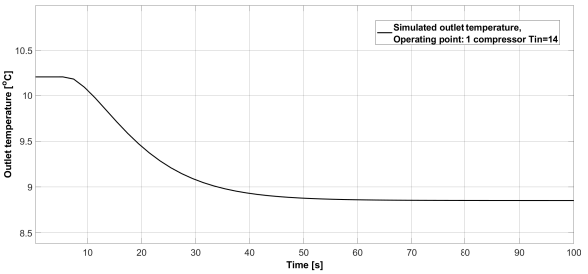

(a) Simulated step response in building 303 VP, static gain $Kp = 10$, time constant $T = 19$, dead time $D = 5$s.

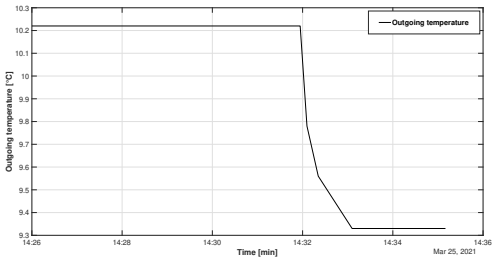

(b) Real step response experiment in building 303, static gain $Kp = 6.4$, time constant $T = 18$, dead time $D = 24$s.

Figure 3.11: A comparison between the simulated step response and a real step response experiment performed in building 303.

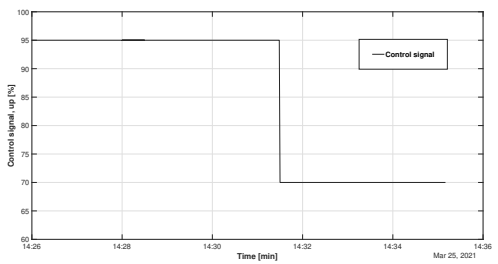

Figure 3.12: Step change in the pump control signal, u_p for the test in building 303.

Temperature-peaks The temperature peak height due to a compressor step was approximately 2 °C, see Figure 3.13. This temperature peak height is compared to a scenario with the old design parameters with a compressor step, see Figure 3.14. It could be concluded from this that the peak height obtained with the new design is not improved. Yet, the control signal for the new design is more aggressive. A higher controller gain would theoretically result in lower peaks due to more control action. But the long measurement delay in the temperature sensor can be an explanation for this. If the time to register a change in temperature is long, the controller will not have time to adjust the flow in time to counteract the temperature change. Thus, a long dead time might be a limiting factor to reduce the peaks with a regular PI.

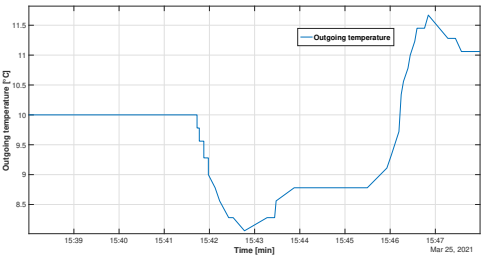

(a) Outlet temperature with new PI-design.

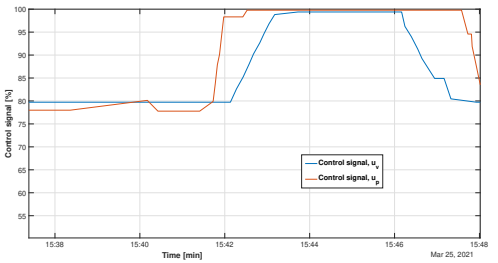

(b) Control signal for pump, u_p and valve, u_v for new PI-design.

Figure 3.13: Temperature peak-height and control signals for the new PI-design caused by a compressor step in building 303 VP. Data extracted from 2021-03-25.

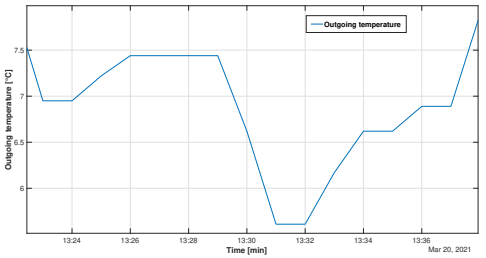

(a) Outlet temperature manually tuned PI.

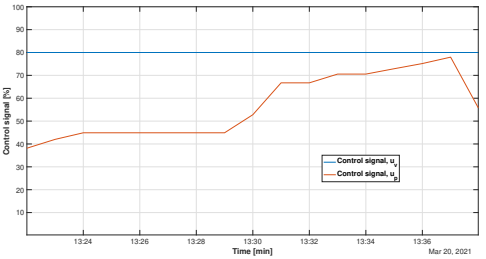

(b) Control signal pump, u_p and u_v for manually tuned PI.

Figure 3.14: Temperature peak-height and control signals for manually tuned PI caused by compressor step in building 303 VP. Data extracted from 2021-03-20.

Stability During the testing of new parameters, the inlet temperature increased, which corresponds to a decreased flow. At this point, the system reached another operating point and the system started to self-oscillate. When this occurred, the test was cancelled due to these oscillations. The self-oscillations was probably related to the new operating point. A lower flow resulted in a longer physical transport delay which might have caused oscillations in the system. The step response and tuning were not performed in the worst case, resulting in a bad design. To receive a robust design, the tuning has to be done at the lowest flow of the system corresponding to the longest dead time.

Temperature Sensors

The long time delay obtained from step response experiment compared to the theoretical means that there is an extra 19 s delay. After some investigation, this delay was assumed to be caused by the temperature sensor. The installed sensor has a time constant of up to 18 s [*Dykgivare med kopplingshus och dykrör* 2021]. Normally, temperature sensors have a high time constant since this usually corresponds to higher accuracy of measurement. Indeed, the time constant of the sensor is a trade-off situation between accuracy and the speed of the sensor to react to fast changes.

The accuracy is often of greater concern which can results in a larger time constant. But in control applications, it is important to be able to react fast to changes in the system. Therefore, it is sometimes desired to improve the time constant of the sensor and a solution to this could be to implement a lead/lag filter, which can help overcome the problems arising from a slow sensor [Hägglund, 2012].

Conclusion from Test in Building 303

- A higher controller gain did not result in lowered temperature peaks. The peaks can not be reduced with a higher controller gain, K. This could be explained by long measurement delays in the temperature sensor.

- The discovered long dead time, D might be a limiting factor in the system regarding control.

- The system is very sensitive for changes in operation point, the system needs more robust controller parameters.

3.6 Impact of Control Parameters

The results from the test underline that it is important to better understand how the controller parameters (gain K and integral time T_i) affect the controlled system. To that extent, in this section, their impact on temperature peaks and stability margins is analyzed thanks to the linearized model of the system Equation 2.18.

To understand the impact of K and T_i's ability to reduce temperature peaks due to compressor steps, the heat transfer, P are considered as a load disturbance. A high ability to suppress the disturbance corresponds to low amplitude between heat transfer and outlet temperature at low frequencies [Åström and Murray, 2008]. This is evaluated by looking at the bode plot (see Figure 3.15) diagram of the transfer function from heat transfer power to outlet temperature, see Equation 2.18 and 2.21. An increased gain results in a decreased amplitude at low frequencies, indicating that the ability to reduce peaks is higher compared to a lower gain. Regarding T_i, a low T_i gave lower amplitude resulting in better disturbance rejection.

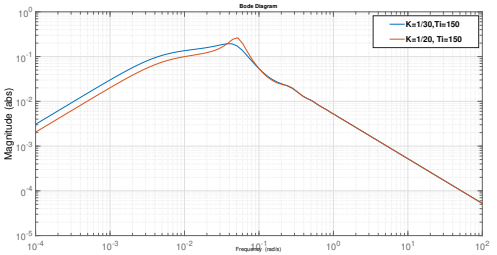

(a) Bode diagrams for different controller gains, K.

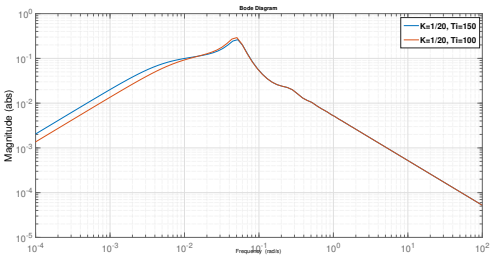

(b) Bode diagrams for different integral times, T_i.

Figure 3.15: Bode diagrams for different values of controller gain, K and integral time, T_i.

Looking at stability margins, such as phase margin φ_m, amplitude margin G_m and delay margin D_m for the open-loop system, these margins increased with a lower gain and increased T_i. This corresponds to the same observations obtained from simulations with different λ, in Figure 3.10. Since the stability is evaluated for the linearized heat pump, it is preferable if the stability margins are large. Indeed the real system contains nonlinearities and unpredicted disturbances which may decrease stability. It is especially important to keep the delay margin of the system higher than the time delay of measurement if the design is only based on physical delay.

3.7 Improved Tuning Method

The analytical investigation shows that there is a trade-off between stability and reducing the peaks when using a PI-controller. Considering the risk of freezing, the peaks cannot be too large if the reference temperature is low. In that case, the temperature risks to go below 4.5 ^{o}C when a compressor is started. It is chosen to keep the lambda-tuning method and to use λ as a tuning parameter to adjust the tuning regarding the peaks. The controller gain is calculated with Equation 3.5. To

increase stability, the integral time was also chosen to be adjusted with a factor x. This is expressed in Equation 3.6.

$$K = \frac{T}{K_p(D+\lambda)} \tag{3.5}$$

$$T_i = xT \tag{3.6}$$

The controller can be designed considering the overall dead time, D of the process based on a step response experiment. If the physical transport delay is known, this can be used for design also, but in this case, the delay margin must be larger than the measurement delay.

3.8 Simulation of Improved Tuning Method

This method is used to tune the controller in building 406. The performance is evaluated according to the section 3.2. Using λ=0.5T, $D = 10$ and $x = 5$ this results in controller parameters of K=1/20 and T_i=100s. The stability margins for the linearized system are considered large enough to keep stability in the system, phase margin $\varphi_m = 67^o$, amplitude margin $G_m = 3.3$ and delay margin $D_m = 33$s. The delay margin indicates that there is room for a measurement delay of 23 s.

The controller is evaluated as described in the section 3.2 and compared to the performance of the old manually tuned PI-design. The result, including outgoing temperature and control signals, is presented below in Figure 3.16-3.19. The ability to reject disturbances from compressor steps is presented in Figure 3.16, disturbances in inlet temperature in Figure 3.17 and flow fluctuations in Figure 3.18. The result for real data is presented in Figure 3.19. The result shows that the peaks are reduced a little bit but with maintained stability.

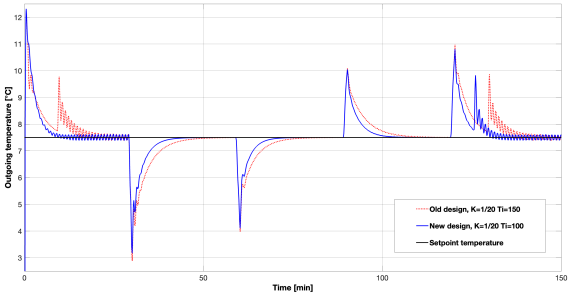

(a) The resulting outgoing temperature of the new designed PI compared to the manually tuned PI.

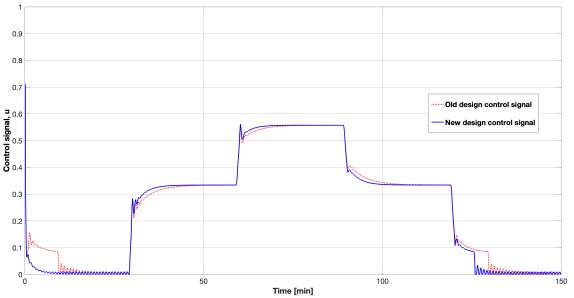

(b) The control signal of the new designed PI compared to the manually tuned PI.

Figure 3.16: Simulated controller performance of outgoing temperature and control signal for the manually tuned PI compared to the new design of the PI when introducing a compressor step.

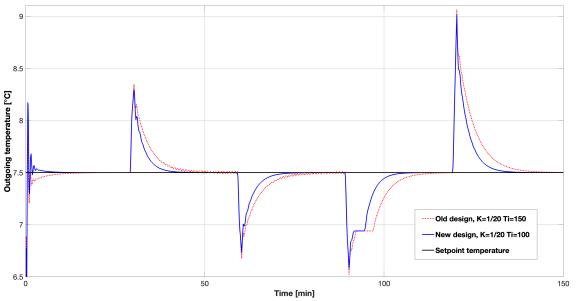

(a) The resulting outgoing temperature of the new designed PI compared to the manually tuned PI.

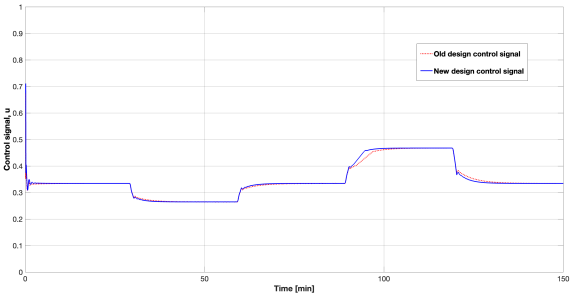

(b) The control signal, u of the new designed PI compared to the manually tuned PI.

Figure 3.17: Simulated controller performance of outgoing temperature and control signal for the manually tuned PI compared to the new design of the PI when introducing a step in inlet temperature.

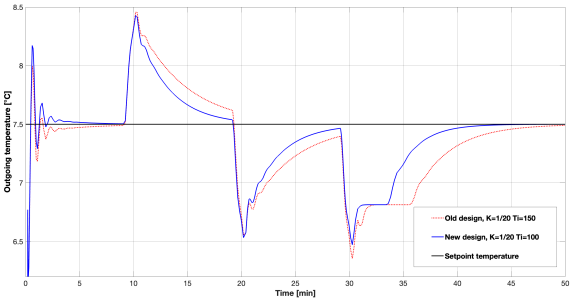

(a) The resulting outgoing temperature of the new designed PI compared to the manually tuned PI.

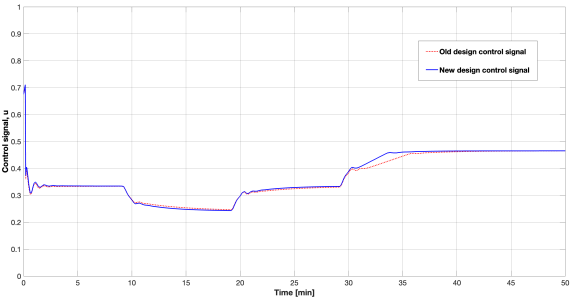

(b) The control signal, u of the new designed PI compared to the manually tuned PI.

Figure 3.18: Simulated controller performance of outgoing temperature and control signal for the manually tuned PI compared to the new design of the PI when introducing flow fluctuations.

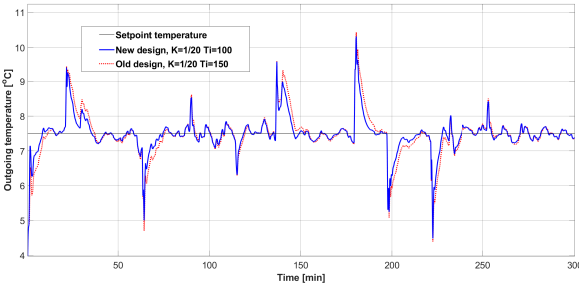

(a) The resulting outgoing temperature of the new designed PI compared to the manually tuned PI.

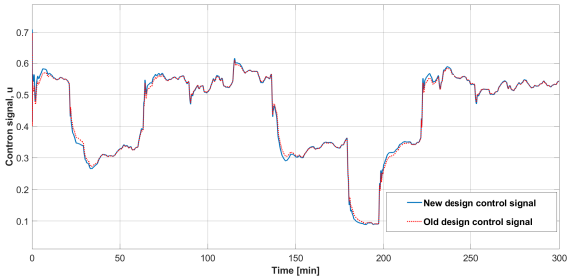

(b) The control signal, u of the new designed PI compared to the manually tuned PI.

Figure 3.19: Simulated controller performance of outgoing temperature and control signal, u for the manually tuned PI compared to the new design of the PI when introducing real data of inlet temperature and heat pump power.

3.9 Verification of New Tuning Method in Building 303

Considering the improved method, this is tested in building 303 for method verification. First, a step response experiment of the system is performed for the worst case (lowest flow and with one compressor in operation). A step in the control signal of the pump, u_p, see Figure 3.20a from 0.3 to 0.7 is done corresponding to a step change in the control signal, u of 0.23. This step change results in an increase in outgoing temperature of 5.1°C. The result from the step response is presented in Figure 3.20b. From the step response the dead time is decided to D=15 s, the time constant, T=30 s. The static gain, Kp is calculated to 22.4.

New PI-parameters are calculated according to equation 3.5 and 3.6 with λ=0.5T and x=4. This results in a K=1/22 and T_i=120s. These parameters are implemented, see Figure 3.21a for performance of new design PI-controller. Data with the manually tuned PI-parameters is presented in Figure 3.21b.

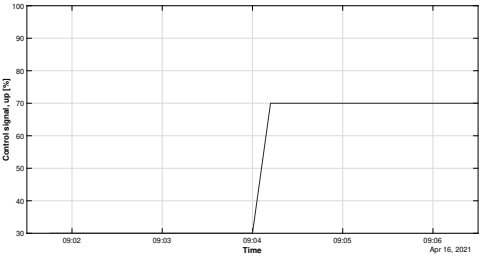

(a) Step change of the control signal of the pump, u_p from 30 to 70%.

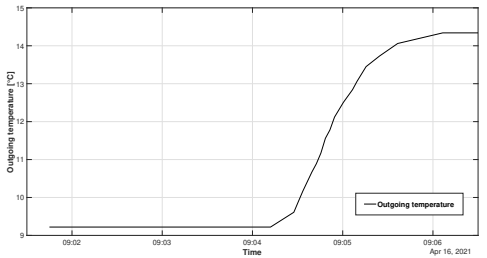

(b) The outgoing temperature after introducing a step change.

Figure 3.20: Step response experiment of building 303 VP used for verification of the improved tuning method.

The verification test of the improved method indicates that the suggested tuning method works on a new building. The method results in parameters with stable control of the system. Temperature peaks >2°C could be avoided and in the meantime maintain desired stability in the system. This design is very similar to the manually tuned design. But, with this method, it is not necessary to manually tune the controller for every energy-sharing module. Instead, the result can be reproduced using the method on other buildings.

Considering the specifications of the new control, this tuning method does not correspond to a improved reduction of temperature peaks. The trade-off between stability and peaks limits the upper value of the controller gain. Also, the long dead time can be a possible explanation for the difficulties of reducing the peaks in outgoing temperature. Therefore, the possibility to reduce the disturbances using a feedforward is discussed in section 4.3.

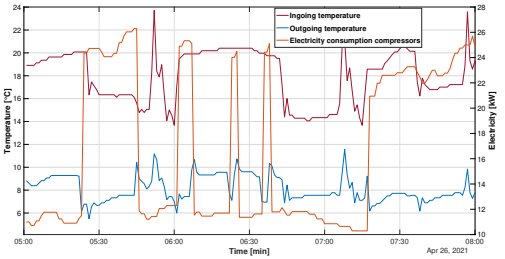

(a) New design PI-parameters.

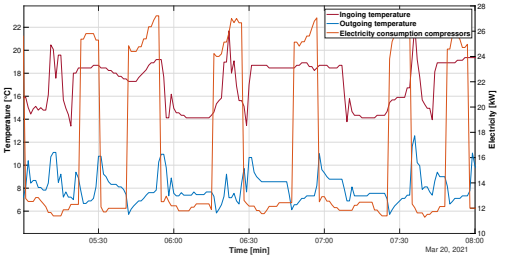

(b) Manually tuned PI-parameters.

Figure 3.21: Comparison between new and manually tuned PI-design parameters in building 303 showing inlet temperature, outlet temperature and electricity consumption in compressors.

4

Conclusions and Outlooks

This project aimed at improving flow control into one energy-sharing module. By using the physical relations between flow, temperature and energy, the flow can be adjusted to meet the specific heating or cooling demand in the building. To maintain high efficiency in ectogrid™ grid temperatures must lie within a specific range. Thus, the controller should reduce the impacts of different disturbances such as variations of inlet temperature, compressor steps and flow fluctuations. This was investigated with a pre-study using a developed model of an energy-sharing module, simulated in Matlab Simulink®. The result from the pre-study was used for support of new controller testing in real buildings. The objective was additionally to develop a way to tune controllers in new buildings. Today, the PI-controllers are manually tuned, which is time consuming and results in different installations between buildings. Therefore, a method was developed resulting in a generic way to tune new buildings ans is detailed in next section.

4.1 Method for Future Controller Tuning

1. Allocation: Adjust the minimum valve opening to reach the lowest required flow in order to reach set-point temperature.

2. Do a step response experiment when one compressor is in operation

    - First, put the controller in manual mode.
    - Make a step-change in u_p, from minimum u_p. Transfer the step-change in u_p to u through the allocation equation.

$$\Delta u = \frac{\Delta u_p}{A} \tag{4.1}$$

      Where A is the allocation factor between u and u_p

    - Read of the process output, this is the outlet temperature.

- Read the new outlet temperature at steady-state and calculate the static gain, $Kp = \frac{\Delta T_{out}}{\Delta u}$
- Read the time constant, T of the process from the graph, when outgoing temperature is 63% of the final value.
- Read the dead time, D from the graph.

3. Calculate PI-design parameters, controller gain K with $\lambda = 0.5T$ and integral time T_i with x=5.

$$K = \frac{T}{Kp(\lambda + D)} \tag{4.2}$$

$$T_i = xT \tag{4.3}$$

The parameters such as, dead time, time constants and static gain can be identified from the step response, see Figure 3.4 in chapter 3. The parameters λ and x, allows the PI-design to be adjusted. This can be evaluated by looking at oscillations and temperature peaks. If the peaks are >2 ^{o}C, λ could be lowered further. If there is no oscillation the factor, x can be reduced to 4 to decrease peaks. If the system tends to be oscillatory, λ can be increased to 1 for more robustness.

4.2 Discussion

A tuning method was developed for controller tuning in new buildings. The main advantage of the proposed controller design is that it provides a generic way to tune controllers in new buildings. The method consists of three steps; determine allocation, performing a step response and finally calculate the controller parameters, K and T_i. The chosen tuning method is based on lambda-tuning method. Normally, lambda-tuning method results in an integral time equal to the time constant of the process. Implementing a design according to traditional lambda-tuning resulted in self-oscillation during the experiment in building 303. This was explained by the long measurement delay in temperature sensors. Therefore, an extra parameter increasing the integral time was introduced. Apart from the integral time parameter, the lambda-tuning method provides an extra tuning parameter, λ to adjust the controller gain. It contributes to an extra degree of freedom when connecting new buildings. All buildings are different in terms of flow capacity, the number of heat pumps and sensor placement. It could therefore be beneficial to adjust the tuning for the current circumstances. Also, strong interconnections between energy-sharing modules contribute to these variations. During this project, only energy-sharing modules equipped with a heat pumps (VP) are investigated. Deviations might appear for the

control of a module with a chiller (KP), where the free-cooling[1] might affect the control performance.

Verification of the tuning pipeline in building 303 resulted in a PI-design similar to the manually tuned controller. The control performance was improved marginally regarding disturbance rejection with the new design. The PI-controller was found to have some limitations considering the peak reduction while maintaining stability. Due to nonlinearities, varying operating points and interconnections in the system the controller should be designed with a highly robust configuration. It is therefore reasonable to assume that an ordinary PI can not meet all specifications. This can be supported by the analytical investigation of the design parameters, K and T_i. A higher controller gain results in a better ability to suppress disturbances in outlet temperature caused by compressor steps. At the same time the stability margins, such as phase margin, amplitude margin and delay margin is decreased with a higher gain. To conclude, to maintain high stability margins the peak reduction is limited.

One part of the tuning method includes determining the allocation of the control signal between the pump and valve. It is of importance that this is done before tuning since this will have an impact on the control. The allocation is essential for determining the available range of flows into an energy-sharing module since the minimum pump speed and valve opening corresponds to the lowest flow in the system. The lowest flow should be equal to the flow needed to reach the set-point temperature with one compressor in operation. During this project, this aspect of the proposed tuning pipeline was highlighted. The allocation configuration needed to be adjusted in building 406, the minimum valve opening was decreased to reach a set-point temperature of 7.5°C to meet the lowest heating demand. The allocation should be chosen to generate a control structure robust against disturbances. This means that the configuration of the pump and valve should allow a flow range wide enough to avoid saturation of the control signal. Another aspect of a robust allocation configuration regards the ability to handle variations of external grid pressure. A large pressure drop over the valve results in a need for a large pressure increase over the pump (see Figure 2.8 in section 2.2). Such configuration makes the flow control less sensitive against variation in the external grid pressure. At the same time, it is a matter of economics. A larger pressure drop over the valve results in higher operating costs since the power consumption of the pump increase with a higher speed. Additionally, it could be preferable if the flow change is linear to the control signal independently on which actuator affecting the flow. Therefore, it would be interesting to investigate how the performance is affected by different allocation strategies.

[1] Free-cooling: Energy of such temperature that it can be used immediately (i.e. without needed any additional work from a heat pump or chiller) through a heat exchanger

In this project the pump and valve work in sequence. The flow control of the pump and valve in parallel could not be modelled. This was due to unknown flow dynamics of the pump and valve in cooperation. The main reason was the lack of information on how the external pressure affects the overall operating point of the pump and valve. Hence, it was not possible to simulate and evaluate different allocation configurations. Future should however investigate this possibility since it is of great potential to develop a better simulation model. Introducing an accurate measurement of the external grid pressure could help the procedure of understanding the flow dynamics. In a case of a better simulation model, the performance of different allocation possibilities could be evaluated further. With a better understanding of the control performance of the pump and valve in cooperation operating cost could be investigated as well.

One part of the thesis involved an investigation of sensor placement related to time delays. The theoretical transport delay was calculated with approximations of pipe diameters, flow rates and distances. This turned out to differ from the dead time from step response experiments in the buildings. The deviation is probably due to a long measurement delay caused by a large time constant in the temperature sensor. During testing of new control parameters, it was observed that a higher gain did not have a large impact on reducing temperature peaks when a compressor starts or stops. Possibly, this can be explained by the long measurement delay. If the time for the measurement signal to reach the controller is long, the performance is reduced. It is therefore recommended to change temperature sensors to decrease measurement delay and investigate the impact of the measurement delay on temperature peaks.

During the project some factors turned out to limit the scope of investigating the flow control into an energy-sharing module. One factor is the simulation model. The model represents a simplified version of the system, especially there are improvements regarding the pump and valve in cooperation. Also, the model of the mixing point and heat pump were simplified, only reflecting the actual heat transferred. To develop the heat pump model, the time for the compressor to start and stop as well as the time for the water to pass the evaporator/condenser could be considered. Another limiting factor was the availability of measurement signals and the possibility to implement new control structures. The focus has been on the already installed PI-controller. But, there are other techniques with great potential to improve disturbance rejection and to find a suitable configuration of the pump and valve. This is discussed in the next section.

4.3 Outlooks

Feedforward

If there are measurable disturbances in a process it is possible to use a feedforward controller to complement the feedback one. The idea is to reject the effect of the disturbance before a control error has even occurred. How early it is possible to measure the disturbance will affect how effective the feedforward filter will be [Åström and Hägglund, 1995]. Used in control of temperatures in buildings, adding a feedforward filter can lower the outlet temperature variations significantly.

In this case, the measured disturbances are the inlet temperature and compressors steps. By introducing a feedforward filter for these disturbances, see Equation 4.4 and Equation 4.5, the impact can be reduced. The control structure for ectogrid™ is described in Figure 4.1. The overall relationship of the outlet temperature from inlet temperature and power is expressed in the Equation 4.6.

$$u_{ff,Tin} = K_{Tin}(T_{in,sp} - T_{in}) \tag{4.4}$$

$$u_{ff,P} = K_P(P - P_0) \tag{4.5}$$

$$\Delta T_{out} = \frac{P_1(s)G_p(s)K_{Tin}(s)A(s) + P_2(s)}{1 + P_1(s)G_p(s)C(s)A(s)}\Delta T_{in} + \frac{P_1(s)G_p(s)K_P + P_3(s)(s)A(s)}{1 + P_1(s)G_p(s)C(s)A(s)}\Delta P \tag{4.6}$$

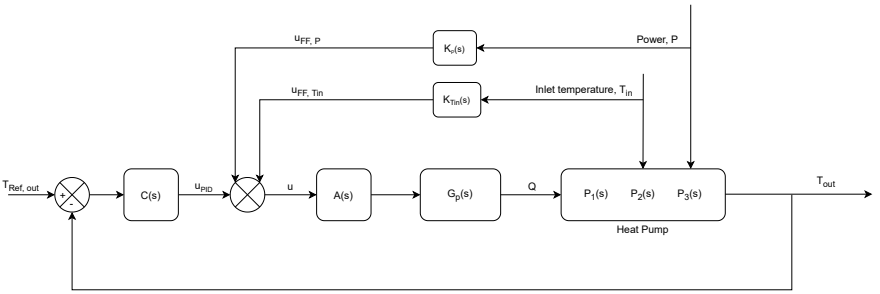

Figure 4.1: A block flow of the system with use of feedforward to compensate for inlet temperature and compressors.

The linearized model of the heat pump is used to calculate the feedforward gains needed to reduce the impact of disturbances, the final expressions of K_{Tin} and K_P

are presented in Equation 4.7 and Equation 4.8, where m_0 and P_0 are stationary parameters corresponding to the worst case. A, is the allocation factor. This resulted in a K_{Tin}=0.02 and K_P=0.0063. The overall control signal is the summary of the control signal from the PI and the two feedforward filters, see Equation 4.9.

$$K_{Tin} = \frac{m_0^2 cp}{P_0 A K_p} \tag{4.7}$$

$$K_P = \frac{m_0}{P_0 A K_p} \tag{4.8}$$

$$u_{tot} = u + u_{ff,Tin} + u_{ff,P} \tag{4.9}$$

The availability and sampling time of the disturbance signal is of great importance for introducing a feedforward. The inlet temperature is sampled with a one second interval and the signal is considered fast enough for use with feedforward. Regarding the compressors steps, a signal implying when a compressor is started or stopped is needed to alter flow accordingly. Currently, there is no signal fast enough to indicate when the compressors are stepping in and out. Therefore, it was assumed that the electricity consumption of the heat pump could be measured with a high resolution and used for feedforward. The relation between heat transfer and power input is related to COP of the heat pump, (see section 2.5).

Introducing the two feedforward gains, this showed good results in terms of reducing the temperature peaks. The simulated outgoing temperature with a feedforward filter of the electricity consumption compared to the result with no feedforward are presented in Figure 4.3. The same comparison but with the inlet temperature as feedforward filter is presented in Figure 4.4. Finally, both feedforward filters are added, see Figure 4.5. In Figure 4.2 data used for simulations is presented. The simulation results, in terms of reducing the peaks, look very good compared to the normal PI-controller. This indicates that this might be a very effective solution to avoid peaks caused by compressor steps.

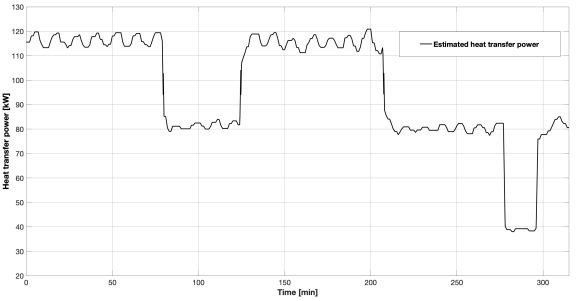

(a) Estimated heat transfer power from electricity consumption heat pump.

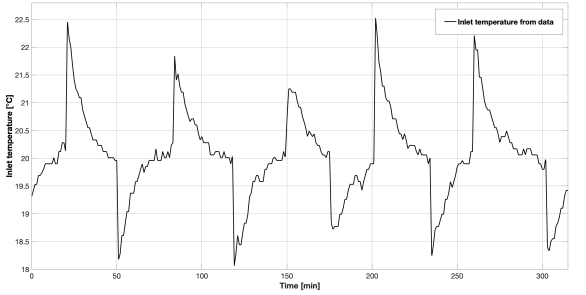

(b) Inlet temperature data.

Figure 4.2: Data used for simulation of feedforward filters. Data extracted from 2021-03-04.

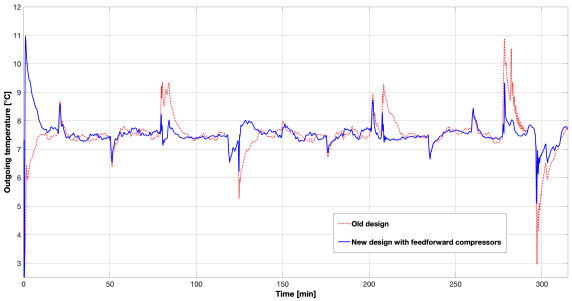

(a) Outgoing temperature

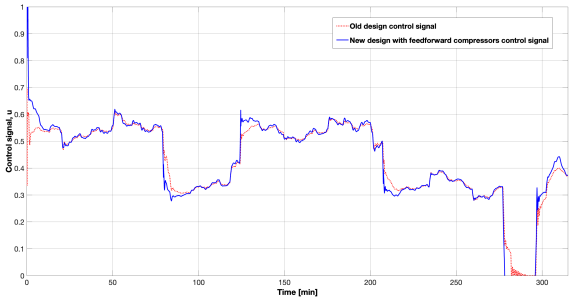

(b) Control signal

Figure 4.3: Results from the simulated feedforward control, compensating for disturbances from compressor steps, compared to the result for an ordinary feedback control.

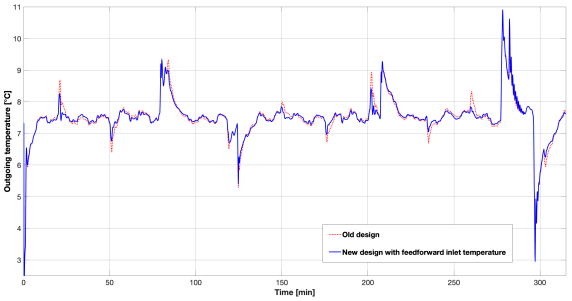

(a) Outgoing temperature

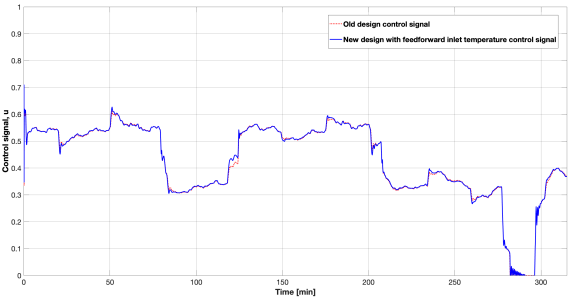

(b) Control signal

Figure 4.4: Results from the simulated feedforward control, compensating for disturbances from inlet temperature, compared to the result for an ordinary feedback control.

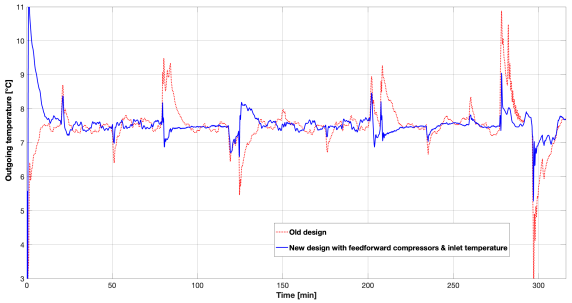

(a) Outlet temperature

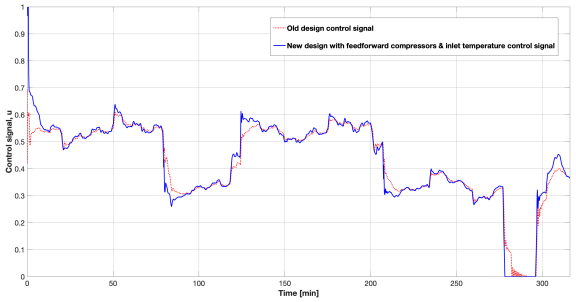

(b) Control signal

Figure 4.5: Results from the simulated feedforward control, compensating for disturbances from compressor steps and inlet temperature, compared to the result for an ordinary feedback control.

Summary of Possible Techniques

In this section, other possible control strategies for controlling the flow with a pump and valve is mentioned. These strategies have been discussed during the project but due to time limitation, this is only mentioned as outlooks. The strategies have good potential and should be further investigated.

Mid-range control The mid-range control strategy is often used when there is more than one actuator controlling one process variable. The principle with mid-range control is that one actuator will be working close to saturation and the other one in its mid-range. The method is therefore often used to decide how the two actuators will cooperate. An example of when the mid-ranging can be utilized is flow control with a pump and valve. This is both economical favourable and energy-saving [Hägglund, 2019a]. Hence, this is a control structure that could be useful in ectogrid™ for control of flow with the pump and valve. As mentioned before, this would need a deeper understanding of the flow dynamics between the circulation pump, control valve and external grid pressure.

Cascade control Cascade control strategy requires access to two measurement signals, creating one fast inner loop and one slower outer loop. The two loops can use simple PID-controllers. Based on a combination of two controllers, the outlet signal from the first is a reference value to the next. One example is the control of a heat exchanger, where the inner loop is controlling the flow with a reference value from the outer loop, temperature signal [Hägglund, 2019a]. In ectogrid™ this could be a possible control strategy using flow and temperature measurement signals in the loop to increase robustness against flow fluctuations caused by variations in external grid pressure.

Tuning of an Energy-Sharing Module with a Chiller

During the project, the scope was limited to the investigation of buildings equipped with heat pumps (VP). A model was created in an early stage even for an energy-sharing module equipped with a chiller (KP). The model is presented in Appendix B. The model needs to be further investigated using electricity consumption for estimation of heat transfer power with COP. Considering the similar dynamics in both VP and KP the suggested tuning pipeline would probably be good even for KP. But, a further investigation should be done. This regarding how the free cooling can affect control in system and control tuning.

4.4 Conclusion

The suggested tuning method provides a way to tune new buildings to the grid, where the tuning method is based on lambda-tuning. Before tuning, the allocation of the control signal between the pump and valve must be determined. To adapt the tuning for different circumstances in different buildings, two tuning parameters can be used to adjust the controller gain and integral time. Stability problems due to nonlinearities and interconnection and long measurement delay in temperature sensors limit the possibility of reducing temperature peaks caused by compressor steps with a ordinary PI-controller. This indicates that a more complex control structure might be necessary. It is also suggested to implement sensors with shorter time constants to improve disturbance rejection. A feedforward filter could be introduced to reduce temperature peaks due to compressor steps or to reduce the effect of the disturbances of inlet temperature. Simulations of the energy-sharing module with a feedforward control indicate that this might be an effective way of reducing the impact of disturbances in outlet temperature.

Bibliography

Åström, K. and T. Hägglund (1995). *PID Controllers: Theory, Design, and Tuning*. English. ISA - The Instrumentation, Systems and Automation Society. ISBN: 1-55617-516-7.

Åström, K. J. and R. M. Murray (2008). *Feedback systems: an introduction for scientists and engineers. [Elektronisk resurs]*. Princeton University Press. URL: http://ludwig.lub.lu.se/login?url=https://search.ebscohost.com/login.aspx?direct=true&db=cat07147a&AN=lub.1965853&site=eds-live&scope=site.

Björkman, A. (2006). *Reglering och stabilisering av malmflöde*. Validerat; 20101217 (root).

Buffa, S., M. Cozzini, M. D'Antoni, M. Baratieri, and R. Fedrizzi (2019). "5th generation district heating and cooling systems: a review of existing cases in europe." *Renewable and Sustainable Energy Reviews* **104**, pp. 504–522. ISSN: 1364-0321. URL: http://ludwig.lub.lu.se/login?url=https://search.ebscohost.com/login.aspx?direct=true&db=edselp&AN=S1364032118308608&site=eds-live&scope=site.

Dykgivare med kopplingshus och dykrör (2021). Regin. URL: https://www.regincontrols.com/globalassets/commerce-assets/documents/tg-dhw3_ps10029_sv.pdf.

Eastop, T. D. and A. McConkey (1993). *Applied thermodynamics for engineering technologists*. Fifth Edition. Longman. ISBN: 0582091034. URL: http://ludwig.lub.lu.se/login?url=https://search.ebscohost.com/login.aspx?direct=true&db=cat07147a&AN=lub.761966&site=eds-live&scope=site.

Ectogrid (2021). *The ectogridtechnology*. URL: http://ectogrid.com/business-customer/. (accessed: 04.28.2021).

Energimyndigheten (2020). *Energiläget 2020*. Technical report. Statens Energimyndighet.

Forslund, G. and J. Forslund (2016). *Bästa inneklimat - Till lägsta kostnad*. Third Edition. AB Svensk byggtjänst. ISBN: 978-91-7333-782-2.

Goppelt, F., T. Hieninger, and R. Schmidt-Vollus (2018). "Modeling centrifugal pump systems from a system-theoretical point of view". In:

Hägglund, T. (2012). "Signal filtering in PID control". *IFAC Proceedings Volumes* **45**:3. 2nd IFAC Conference on Advances in PID Control, pp. 1–10. ISSN: 1474-6670. DOI: https://doi.org/10.3182/20120328-3-IT-3014.00002. URL: https://www.sciencedirect.com/science/article/pii/S1474667016309922.

Hägglund, T. (2019a). *Praktisk processreglering*. Studentlitteratur. ISBN: 9789144130668. URL: http://ludwig.lub.lu.se/login?url=https://search.ebscohost.com/login.aspx?direct=true&db=cat07147a&AN=lub.5445643&site=eds-live&scope=site.

Hägglund, T. (2019b). "The one-third rule for PI controller tuning." *Computers and Chemical Engineering* **127**, pp. 25–30. ISSN: 0098-1354. URL: http://ludwig.lub.lu.se/login?url=https://search.ebscohost.com/login.aspx?direct=true&db=edselp&AN=S0098135419300626&site=eds-live&scope=site.

Handbook: Physical properties, correlations and equations in chemical engineering. (2019). Department of Chemical Engineering, Faculty of Engineering, Lund University. URL: http://ludwig.lub.lu.se/login?url=https://search.ebscohost.com/login.aspx?direct=true&db=cat07147a&AN=lub.6367407&site=eds-live&scope=site.

Hieninger, T., F. Goppelt, R. Schmidt-Vollus, and E. Schlücker (2021). "Energy-saving potential for centrifugal pump storage operation using optimized control schemes." *Energy Efficiency (1570646X)* **14**:2, pp. 1–14. ISSN: 1570646X. URL: http://ludwig.lub.lu.se/login?url=https://search.ebscohost.com/login.aspx?direct=true&db=a9h&AN=148638638&site=eds-live&scope=site.

Panagopoulos, H., T. Hägglund, and K. Åström (1997). *The Lambda Method for Tuning PI Controllers*. English. Technical Reports TFRT-7564. Department of Automatic Control, Lund Institute of Technology (LTH).

Rezaie, B. and M. A. Rosen (2012). "District heating and cooling: review of technology and potential enhancements". *Applied Energy* **93**. (1) Green Energy; (2)Special Section from papers presented at the 2nd International Enery 2030 Conf, pp. 2–10. ISSN: 0306-2619. DOI: https://doi.org/10.1016/j.apenergy.2011.04.020. URL: https://www.sciencedirect.com/science/article/pii/S030626191100242X.

Team, C. W., R. Pachauri, and L. Meyer (2014). *Climate Change 2014: Synthesis Report. Contribution of Working Groups I, II and III to the Fifth Assessment*

Report of the Intergovernmental Panel on Climate Change. Technical report 151pp. IPCC.

Trüschel, A. (2002). *Hydronic heating systems : the effect of design on system sensitivity.* Doktorsavhandlingar vid Chalmers tekniska högskola: Ny serie 1857. Chalmers tekniska högsk. ISBN: 9172911751. URL: http://ludwig.lub.lu.se/login?url=https://search.ebscohost.com/login.aspx?direct=true&db=cat07147a&AN=lub.1449158&site=eds-live&scope=site.

Ventilställdon M400 (2008). inu. URL: https://inu.se/Portals/0/Documents/Datablad/Ventilmotorer/M400.pdf.

Ventilställdon M800 (2010). Tornlinds. URL: http://www.tornlinds.se/assets/m800-st%C3%A4lldon.pdf.

Yu, C.-C. and s. SpringerLink (Online (2006). *Autotuning of PID Controllers. [electronic resource] A Relay Feedback Approach.* Springer-Verlag London Limited. ISBN: 9781846280368. URL: http://ludwig.lub.lu.se/login?url=https://search.ebscohost.com/login.aspx?direct=true&db=cat07147a&AN=lub.5727395&site=eds-live&scope=site.

A

Matlab Simulink®

Figure A.1 shows the model of an energy-sharing module in Matlab Simulink®. The control error, which is the difference between set-point temperature and measured outlet temperature enters the PI-controller, generating a control signal. The control signal is allocated between the two actuators, the circulation pump and control valve, which results in a flow. Further, the flow enters the heat pump together with inlet data for inlet temperature and electricity consumption (which is transferred to heat transfer power via COP). This results in an overall outgoing temperature, which is delayed with the physical transport delay through pipes. The models describing the the included components (PI-controller, circulation pump, control valve and heat pump) are described in more detail in chapter 2.

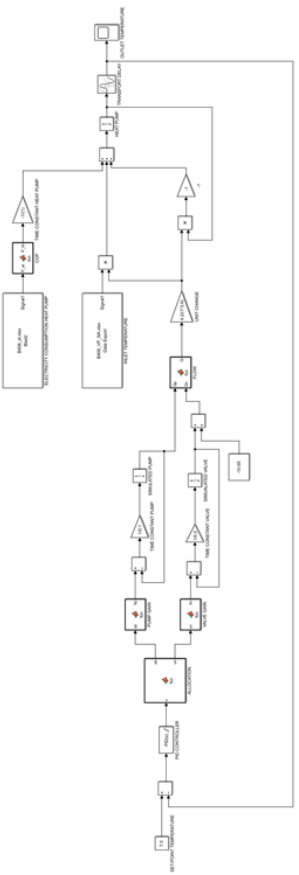

Figure A.1: Simulink® model of one energy-sharing module. The model includes a PID-controller with allocation of the control signal to the circulation pump and control valve, the simplified heat pump with inlet temperature and electricity consumption as input signals and finally the physical transport delay.

B

Simulation Model of an Energy-Sharing Module with a Chiller

The developed model of an energy-sharing module with a chiller in building 406 is presented in this appendix. The plotted flows as a function of the control signal of the pump and valve are presented in Figure B.1 and B.2.

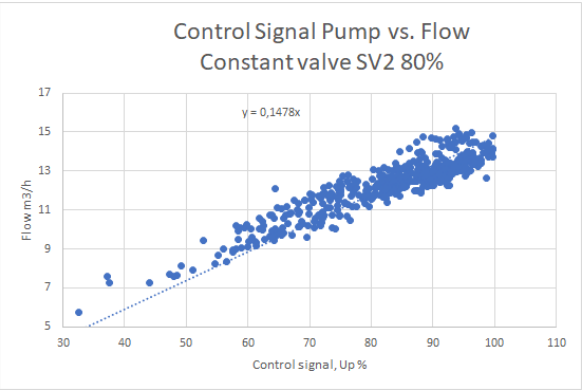

Figure B.1: Control signal for the pump as a function of flow with linear regression $Q = 0.15u_p$. Data extracted from 2020-05-15, 2020-07-04, 2020-08-20, 2020-09-11, 2020-09-12 and 2020-11-04.

The resulting pump gain, K_p for different regions of the control signal, u_p is presented in Table B.1. The valve gain, K_v was estimated to 0.2. PI-parameters for the manually tuned PI is presented in Table B.2 and the allocation of the control signal

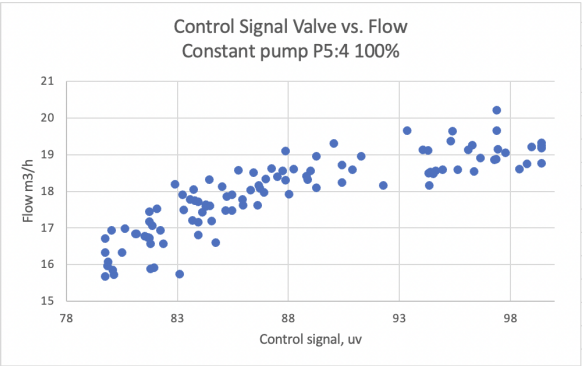

Figure B.2: Control signal for the valve as a function of flow. Data extracted from 2020-04-13, 2020-06-01, 2020-06-02, 2020-06-05, 2020-06-11, 2020-06-25, 2020-06-26, 2020-07-02 2020-07-03.

between the circulation pump and control valve in Table B.3. The resulting simulated closed-loop compared to real data is presented in Figure B.3, showing the simulated outlet temperature and flow. The set-point temperature is 20°C. Data for inlet temperature, power and control signal is presented in Figure B.4.

Table B.1: Resulting pump gain, K_p in different regions of the control signal.

KP	
K_p	u_p
0.16	$u_p < 0.55$
0.15	$u_p > 0.55$

Table B.2: The manually tuned PI-parameters for KP

PI-Parameters	
K	T_i
1/20	300

Table B.3: Allocation for KP in B406

B406 KP		
u_{PID}	u_{Pump}	u_{valve}
$u < 0.45$	1	$1 - 4/9u$
$0.45 < u < 0.5$	1	0.8
$u > 0.5$	$1.7 - 1.4u$	0.8

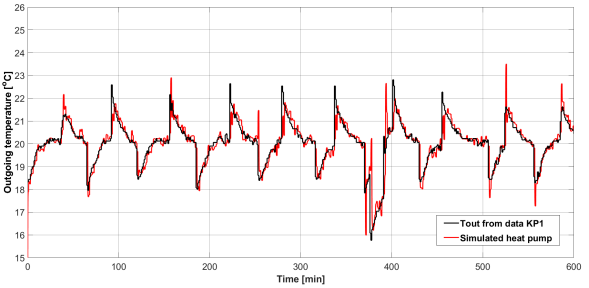

(a) Outgoing temperature compared to measurement data. Data extracted from 2021-01-21.

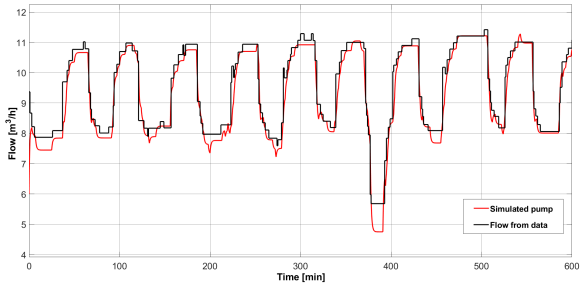

(b) Flow compared to measurement data. Data extracted from 2021-01-21.

Figure B.3: Simulated results of outgoing temperature and flow for the closed loop compared to measurement data extracted from ectocloud™.

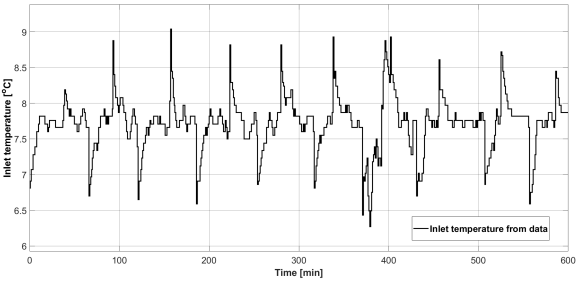

(a) Inlet temperature from data. Data extracted from 2021-01-21.

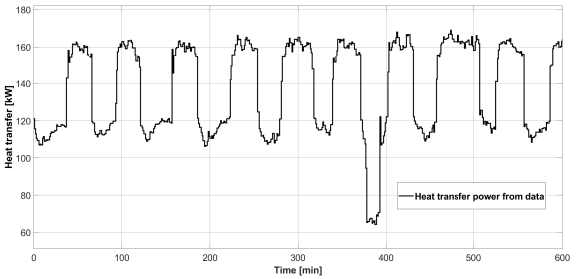

(b) Heat transfer power from data. Data extracted from 2021-01-21.

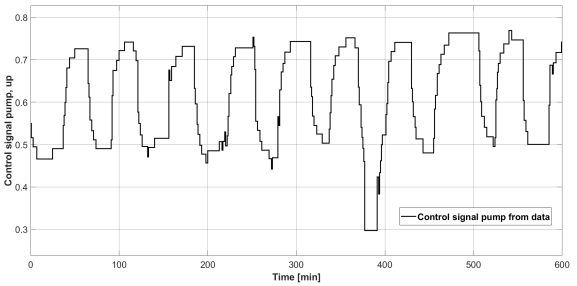

(c) Control signal of the pump compared to measurement data. Data extracted from 2021-01-21.

Figure B.4: Extracted data of inlet temperature, heat transfer and control signal of the pump used in simulations of the closed loop system.

C

Project activities

During the project, a number of project activities was performed. In this part of the appendix, these activities are presented, including the purpose of the activity and a list of people that attended.

C.1 Workshop 16/3-2021

The workshop was held in the middle of the project with the purpose to get input on the work so far and discuss further work. For the workshop people from both the Automatic Control Department at LTH and E.ON.- ectogrid™ was gathered. The following people attended:

- Daniel Stenberg
- Felix Agner
- Jacob Skogström
- Karl-Johan Åström
- Pauline Kergus
- Per Rosén
- Thomas Ranstorp
- Tore Hägglund

C.2 Testing in Real Buildings

Building 303 25/3-2021

The purpose of the activity was to do a step response experiment in building 303 for comparison of the created model used in Matlab Simulink®. At the time also

new parameters were tested to evaluate the tuning method. The people that attended were Thomas Ranstorp and Daniel Stenberg.

Building 406 8-9/4-2021

The purpose of the activity was to do a step response experiment in building 406 to investigate the discovered long dead time. But also, try new PI-parameters with the tuning method. The people that attended were Thomas Ranstorp and Daniel Stenberg.

Building 303 16/4-2021

The purpose of the activity was to test the improved tuning method again on a different building to verify the method. The people that attended were Thomas Ranstorp and Daniel Stenberg.

Nomenclature

ρ	Density [kg/m^3]
λ	Closed loop time constant for Lambda-tuning
τ	Normalized time-delay
φ_m	Phase margin [°]
$A(s)$	Allocation factor
A_C	Cross sectional area pipe [m^2]
$C(s)$	Transfer function PI-controller
COP	Coefficient of performance
d	Pipe diameter [m]
D_m	Delay margin [s]
Dm	Dead time caused by measurement delay
Dt	Dead time caused by physical transport of water
G_m	Gain margin
$G_p(s)$	Transfer function pump
$G_v(s)$	Transfer function valve
K	Controller gain
K_P	Feedforward gain compressors
K_p	Pump gain
K_v	Valve gain

k_v Valve capacity coefficient

K_{Tin} Feedforward gain inlet temperature

Kp Static gain

m_0 Stationary mass flow [kg/s]

$P-band$ Controller P-band [°C]

P_0 Stationary heat transfer power [kW]

$P_1(s)$ Transfer function from flow to outlet temperature in heat pump

$P_2(s)$ Transfer function from inlet temperature to outlet temperature in heat pump

$P_3(s)$ Transfer function from heat transfer to outlet temperature in heat pump

$P_{external}$ External grid pressure[kPa]

P_{pump} Pressure increase by the pump [kPa]

P_{valve} Pressure drop over the valve[kPa]

Q Flow rate [m^3/h]

Q_p Flow in pump

Q_v Flow in valve

s Pipe distance [m]

T Time constant of process

T_i Integral time [s]

T_i Integral time

T_p Time constant pump

T_v Time constant valve

T_{in} Inlet temperature[°C]

T_{out} Outgoing temperature [°C]

u Total control signal

u_p Control signal Pump

u_v Control signal Valve

$u_{ff,P}$	Feedforward control signal compressors
$u_{ff,Tin}$	Feedforward control signal inlet temperature
u_{tot}	Control signal from PI-contoller and feedforward
v	velocity [m/s]
W	Electricity [kW]
x	Factor for integral time

Lund University
Department of Automatic Control
Box 118
SE-221 00 Lund Sweden

Document name
MASTER'S THESIS

Date of issue
June 2021

Document Number
TFRT-6131

Author(s)
Lisa Korsell
Tuva Ydén

Supervisor
Felix Agner, Dept. of Automatic Control, Lund University, Sweden
Pauline Kergus, Dept. of Automatic Control, Lund University, Sweden
Anders Rantzer, Dept. of Automatic Control, Lund University, Sweden (examiner)

Title and subtitle

Control Design for an Energy-Sharing Module of Next-Generation Thermal Energy System ectogrid™

Abstract

Today, heat and electricity production are two main sources of greenhouse gas emissions. A big share of the overall energy consumption is used to provide buildings with heating and cooling. Smart-energy solutions of heating and cooling could therefore be a more sustainable solution contributing to the green transition of the energy system. ectogrid™ is a new generation of a cooperative heating and cooling network providing buildings with energy in an efficient way. Compared to traditional energy solution such a district heating and heat pump/chillers, ectogrid™ is a smart-energy solution utilizing low-temperature heat which is usually wasted.

Every building connected to ectogrid™ has its own production module equipped with a heat pump or a chiller supplying the building with heating or cooling. To meet the required demand in the buildings and to maintain desired grid temperatures, the flow of water from the grid into each building is controlled using a circulation pump and control valve. The network consists of an interconnection of energy-sharing modules affecting each other, therefore it is of importance that the grid temperature lies within a defined temperature range for the network to work efficiently. Today, flow control into a module is currently done using a manually tuned PI-controllers. The objective of this thesis is to improve flow control into one energy-sharing module and to develop a method to tune the controllers for new buildings.

A simulation model over one energy-sharing module equipped with a heat pump was developed using Matlab Simulink®. The model was used as a pre-study for evaluating control tuning methods. Control performances were evaluated on the controller's ability to reject disturbances affecting outgoing temperature as well as the overall stability. The result from the pre-study was used as support for controller testing in real buildings. This resulted in a generic way to tune new buildings connected to the grid, based on lambda-tuning method. The PI-controller is limited regarding disturbance rejection while maintaining stability. Therefore, the possibility to implement a feedforward was investigated using the simulation model. Since feedforward showed great potential in reducing the impact of disturbances this was suggested as a future outlook.

Keywords

Classification system and/or index terms (if any)

Supplementary bibliographical information

ISSN and key title
0280-5316

ISBN

Language
English

Number of pages
1-92

Recipient's notes

Security classification